MECHANISMS OF LASER-SURFACE INTERACTIONS

By

J. F. Ready

E. Bernal G.

L. T. Shepherd

FINAL REPORT

TO

Ballistic Research Laboratories

Aberdeen Proving Ground, Maryland

Contract No. DA-18-001-AMC-1040(X) Modification No. 1

May, 1968

Presented by

Honeywell Inc.

CORPORATE RESEARCH CENTER

Hopkins, Minnesota

DISCLAIMER NOTICE

THIS DOCUMENT IS BEST QUALITY PRACTICABLE. THE COPY FURNISHED TO DTIC CONTAINED A SIGNIFICANT NUMBER OF PAGES WHICH DO NOT REPRODUCE LEGIBLY.

MECHANISMS OF LASER-SURFACE INTERACTIONS

By

J. F. Ready

E. Bernal G.

L. T. Shepherd

FINAL REPORT

To

Ballistic Research Laboratories

Aberdeen Proving Ground, Maryland

Contract No. DA-18-001-AMC-1040(X) Modification No. 1

May, 1968

Presented by

Honeywell Inc.

CORPORATE RESEARCH CENTER

Hopkins, Minnesota

ABSTRACT

This report describes extensions of measurements of particle emission produced in the interaction of high power laser radiation with absorbing surfaces. Most of the experimental work in this report period involved the use of a hemispherical interaction chamber with collectors around the periphery. A multiplier detector and a bipolar detector have been employed in addition to the ordinary disc collectors used previously. The experimental results for a tungsten target and a laser flux density of the order of 50 megawatts/cm^2 indicate that the blowoff material consists of a mixture of neutral molecules and of a plasma containing approximately 10^{13} to 10^{14} electons and ions. Secondary electron emission from the collector surfaces bombarded by the incident heavy particles is important in producing the observed signals. Temperature of the expanding material is of the order of 10 eV. Additional work has been devoted to measuring the optical emission from glass samples heated by a CO_2 laser beam and also to an investigation of the possible presence of picosecond pulses in our laser output.

TABLE OF CONTENTS

LIST OF ILLUSTRATIONS

SECTION I

INTRODUCTION

The investigations described in this report are continuations of work which was carried out previously. The earlier investigations were concerned with particle emission produced in laser-surface interactions and have been described in detail in previous reports (1-6). Some knowledge of the background of this work, as discussed in the previous reports, is necessary for an understanding of the methods and aims of the investigations discussed in the present report. A time-of-flight spectrometer has been used to measure ion emission produced by the interaction with metallic targets of ruby laser radiation with flux densities of the order of 50 MW/cm^2. The ions were found to be mainly alkali metals with energies of the order of several hundred electron volts. The neutral molecule emission produced under similar conditions was studied with a quadrupole mass spectrometer and found to consist of thermally desorbed gases such as H_2, CO, and CO_2 along with pulses of high energy neutral molecules having energies of the order of 100 eV.

Additional studies were performed in an interaction chamber, which has the laser-illuminated target at its center, with shielded disc collectors around the periphery of the hemisphere.[4] Measurements of the angular distribution indicated that there is a maximum in both the number of emitted particles and their energies in a direction normal to the target surface, and that both these quantities decrease as the angle from the normal increases. Moreover, the distribution in the plane defined by the direction of the laser beam and the normal to the target surface was different from the distribution in the perpendicular plane.[6]

The present report is mainly concerned with extension and analysis of the measurements performed in the interaction chamber. The measurements performed earlier had some puzzling features. The original philosophy of the design of the hemispherical interaction chamber was that it was intended to measure ionic emission, which had been determined from measurements in the time-of-flight spectrometer to consist mainly of alkali metal ions. It has become apparent that the measurements are also affected by other types of laser-produced particle emission. In addition to direct collection of positive ions produced in the laser-surface interaction, secondary electron emission produced at the collector surfaces when the heavy particles trike the collectors is important.

In order to arrive at these conclusions, we modified the system by adding a multiplier collector along the normal to the target surface in place of one of the original disc collectors. We also used a bipolar collector, which is capable of separating electronic and ionic charge in the blowoff material and measuring them separately. The bipolar collector is not struck by particles traveling directly from the target, but relies on application of a voltage to produce charge separation in the plasma. The results obtained in the bipolar collector indicate a larger amount of ion production than we deduced from the measurements on the time-of-flight spectrometer.

A considerable portion of this report is devoted to analysis and interpretation of these results. A more complicated range of phenomena was encountered than was anticipated in the original design of the hemispherical interaction chamber. However, we feel that the operation of this chamber is better understood than previously.

The present interpretation includes a plasma of electrons and ions in approximately equal numbers plus neutral molecules that travel together in the blowoff material. The average temperature of this material is of the order of 10 eV. The observed signals at the collectors are strongly influenced by the phenomenon of secondary emission. The range of the ionic emission is large enough that it should be necessary to reconsider the inverse Bremsstrahlung mechanism for heating of the blowoff material.

The results obtained in this system are compared to the results from the time-of-flight spectrometer. There are discrepancies which we have not yet resolved.

In addition, the work has been extended into different areas than previously. We have begun experiments involving the interaction of radiation from a carbon dioxide laser. The optical emission from the material evaporated by the carbon dioxide laser has been examined. This work is still in a relatively early stage, but the use of carbon dioxide lasers, particularly in a repetitively pulsed mode, appears promising in these studies.

We have also begun an experiment to determine the possible existence of picosecond pulses in our laser output. Other workers have observed that the output of a Q-switched laser under a very wide variety of conditions is made up of a train of mode-locked pulses, each having a duration of the order of picoseconds. If this situation occurs in our laser, it will have a bearing on previous interpretations of the experiments. Therefore, we have begun an experiment to determine if high frequency pulsation is present under the pulse envelope of our 35 nanosecond duration Q-switched laser pulse.

In addition, the presence of picosecond pulses has implications for the mechanism of damage produced by laser beams in transparent materials. Quantitative estimates of the damage threshold, using the generally accepted mechanisms for damage, have not produced agreement with observed thresholds. If picosecond pulses are present, this discrepancy could possibly be resolved. Therefore, we have begun some preliminary work on the damage of transparent materials.

Section II deals with the work in the hemispherical interaction chamber. Section III describes the work using the carbon dioxide laser, and Section IV is devoted to the subject of picosecond pulses.

SECTION II

THE HEMISPHERICAL INTERACTION CHAMBER

Studies involving the hemispherical interaction chamber, the construction of which was described in detail in the December 1966 report,[4] include experimental work in which different types of detectors were added to the system, and an analysis of the data from the system, in which we attempt to interpret the various types of measurements and to compare them to earlier results.

A. EXPERIMENTAL

In all the experimental work described in this subsection, a tungsten target was employed, and the laser flux density at the target was in the range 50 to 100 megawatts/cm^2.

1. General

In the last semi-annual report[6] we commented on the considerable amounts of noise in the form of high frequency oscillations which were often present in the output signals from the hemispherical interaction chamber. In particular, when the laser beam was in the plane containing the detectors, the noise was most pronounced. In this configuration the laser beam entered a hole in the hemisphere in which a detector had originally been installed. We removed the detector but left the grid which insured continuity of the field at the hemisphere. When this grid was removed so that it was not struck by the incident laser beam, the noise was considerably reduced. In addition, when the plane containing the laser beam and the normal to the target surface was perpendicular to the plane containing the detectors, the laser beam reflected from the target would strike the inside of the hemisphere. After a number of

shots, a visibly damaged spot appeared on the hemisphere at this point. We drilled a hole through the hemisphere at this point in order to allow the beam to exit from the system after striking the target and being reflected without further interactions. Emission of electrons from this point when it was struck by the laser beam may also have contributed to the noise. These measures to insure that the laser beam has a clear access to the target and exit from the system, with no possibility of particle emission from other portions of the system, has solved the noise problem.

There has been considerable difficulty in obtaining good reproducible data from this system, especially in the matter of correlating the outputs with the amplitude of the laser pulse. For a given laser pulse the size of the signal may vary considerably, and if the output is plotted as a function of laser monitor pulse size there is much scatter in the data. Figure II-1 shows such data for a collector at 15° to the target normal. In order to determine definitely the effects of various experiments in the system, it has been necessary to accumulate a large number of data shots, alternating between different conditions of the variable under investigation. For example, if we were investigating the effects of applying a voltage at a certain position in the system, we would take alternate shots with the voltage on and off, in order to separate the effect of the voltage from scatter in the pulse size. Often many shots were necessary to effect the separation.

During the course of these measurements, a hitherto unreported effect was noted on the side of the ruby rod. A series of small cracks began to form on the side of the rod adjacent to the flashtube. See Figure II-2. The damage had the appearance of a white powder-like coating. It can be removed by turning the rod on a small lathe with diamond grit compound, but after further use additional cracking is evident. The presence of the cracking

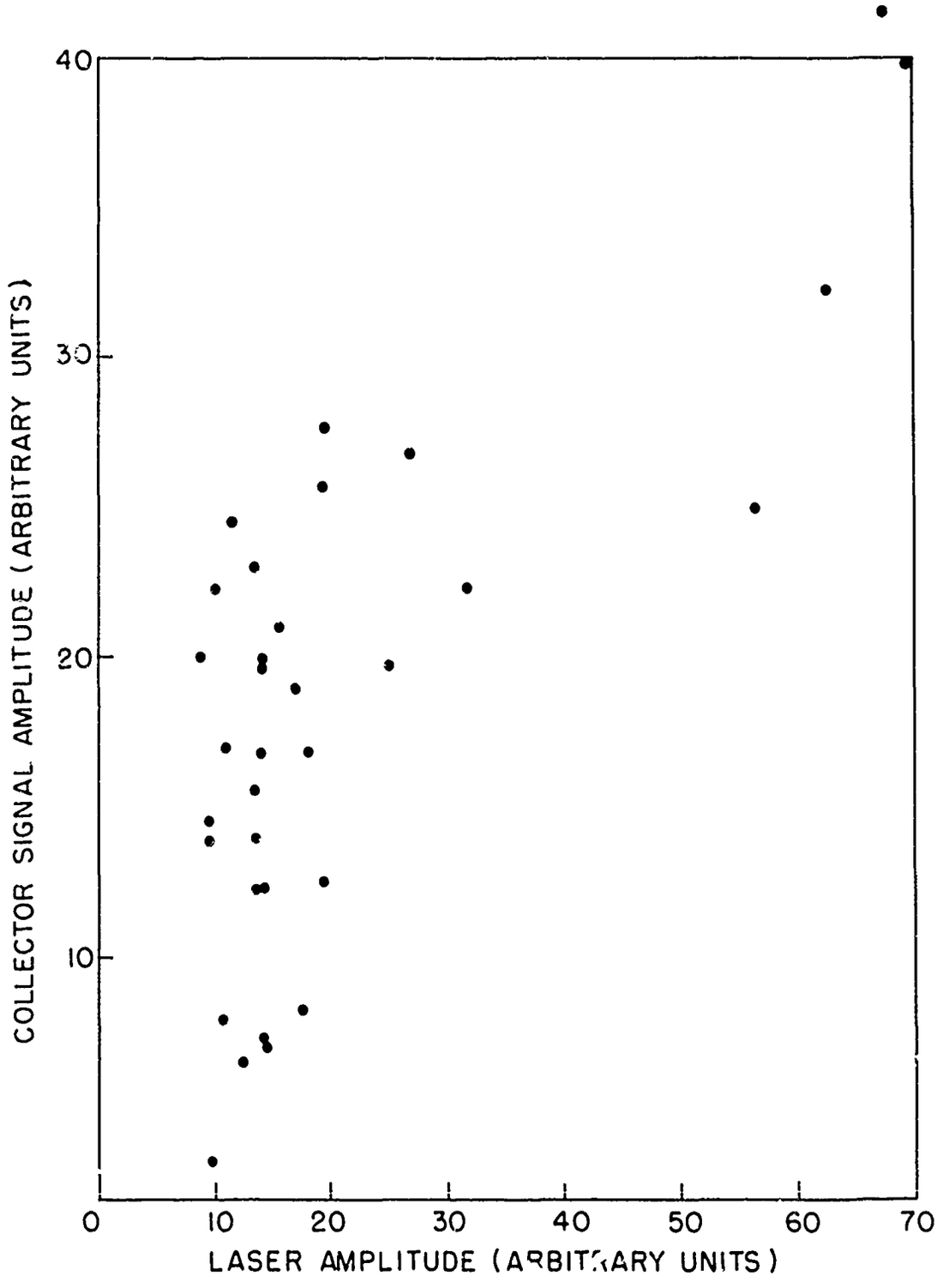

Figure II-1. Scatter in Data From the Hemisphere. The Points Represent Collector Signal Amplitudes Associated with Various Laser Monitor Pulse Heights.

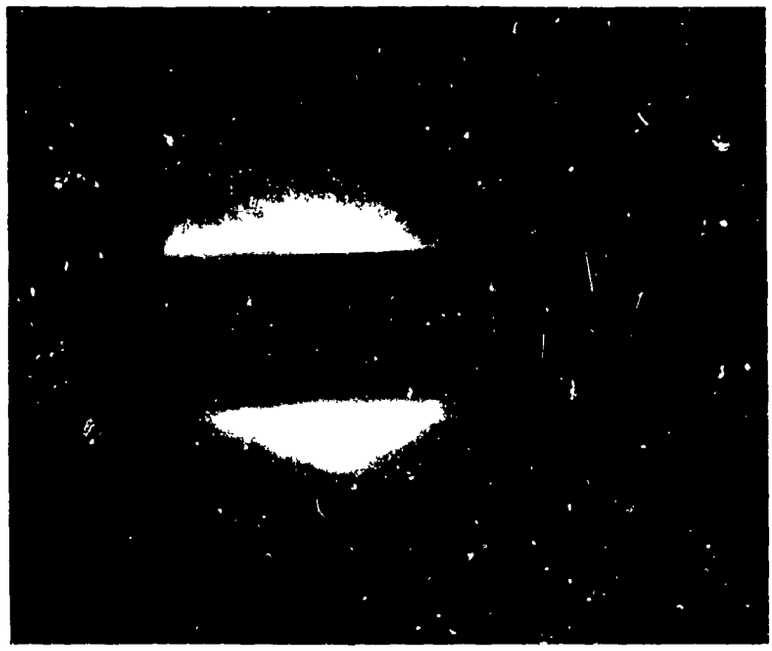

Figure II-2. Photograph of Cracking Along the Sides of a Ruby Laser Rod.

reduces the pump light intensity so that the laser output is reduced. The form of the damage is as shown in Figure II-3. From the appearance of this damage, we feel that it may be caused by absorption in a thin layer at the surface of the ruby. Such absorption may be caused, for example, by small amounts of the polishing compound embedded in the surface of the ruby. Local heating under the action of the pump light would cause expansion and contraction of the surface layer, eventually leading to chipping and flaking of the layer. The damage appears as cracks oriented at 60° to the rod axis, the same direction as the c-axis of the rod, and appears to be consistent with cracking along a crystalline axis of the ruby.

The solvent used to dissolve the cryptocyanine in the Q-switching cell has previously been methanol. During operation of the laser, the solution becomes degraded after a number of shots. In order to restore the output of the laser to its original level, the contents of the passive Q-switching cell must be replaced with a freshly prepared solution. This procedure is somewhat tedious since it involves dripping concentrated cryptocyanine into the cell, drop by drop, and observing the gradual decrease in the number of spikes in the laser output until finally a stable region with a single high power spike is reached. In order to increase the length of service of a given solution, we tried the use of the solvent acetonitrile in place of methanol. There had been reports that operation with acetonitrile gave a Q-switching solution less subject to degradation. We found that it was more difficult to obtain a stable region of operation in which a single spike of approximately constant power level would be produced, with acetonitrile as the solvent. When the laser did emit a single pulse, the amplitude was more variable than when methanol was used as a solvent. In addition, the use of acetonitrile did not significantly improve the length of service of the solution. Therefore, our conclusion is that in spite of reports to the contrary, the use of acetonitrile does not offer any advantage over the use of methanol as a solvent for the bleachable Q-switching dye.

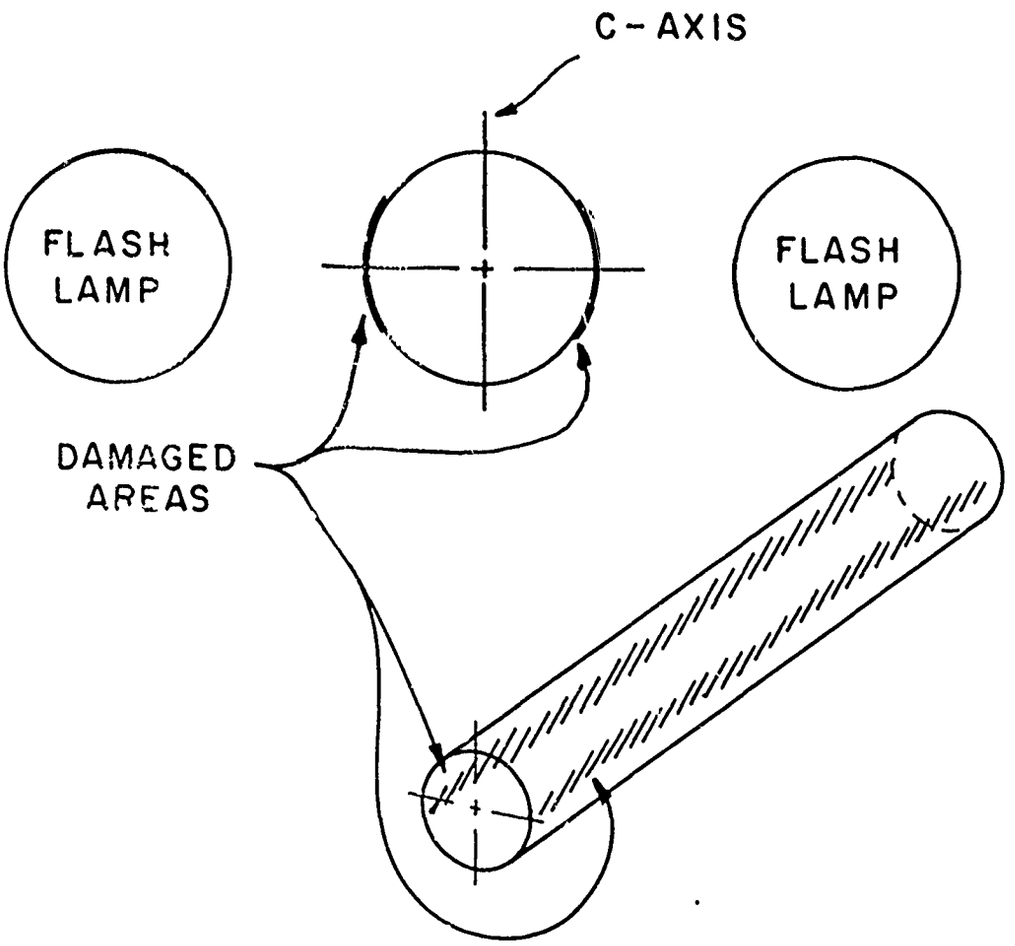

Figure II-3. Drawing of Damage Along the Sides of a Ruby Laser Rod.

2. Angular Distribution

In the last semi-annual report[6] data were presented for the angular distribution of the emission reaching the collectors. The data were presented for two planes: the plane containing the laser beam and the target normal, and also the plane perpendicular to the plane containing the laser beam and the target normal. The previous data were taken with the polarization of the laser beam in the plane containing the incident laser beam and the target normal. There is another possible orientation of the direction of polarization of the laser beam, and as before, two possible planes in which the emission can be measured. The situation is illustrated in Figure II-4. We have obtained data for the case where the polarization of the laser beam is perpendicular to the plane containing the normal to the target and the beam. Some of these data are presented in Figure II-5 which gives the angular distribution in the plane containing the laser beam and the target normal.

These results were obtained by photographing the output of a given collector and of the collector along the target normal (#6) on a dual beam oscilloscope. The data plotted are the ratios of the signal (the integrated area under the curve) from the given collector to the signal from collector #6 for each shot. The data at 90° are thus normalized to unity. Even with such normalization, which should tend to remove the effect of varying laser flux density from shot to shot, there still is considerable scatter. The general trend of the data is clear, however. No measurable signals were obtained from the two collectors at 75° to the target normal.

These results may be compared to Figure II-8 of the last semi-annual report which for completeness is reproduced here as Figure II-6. The plane in which the present angular distribution was measured was the same

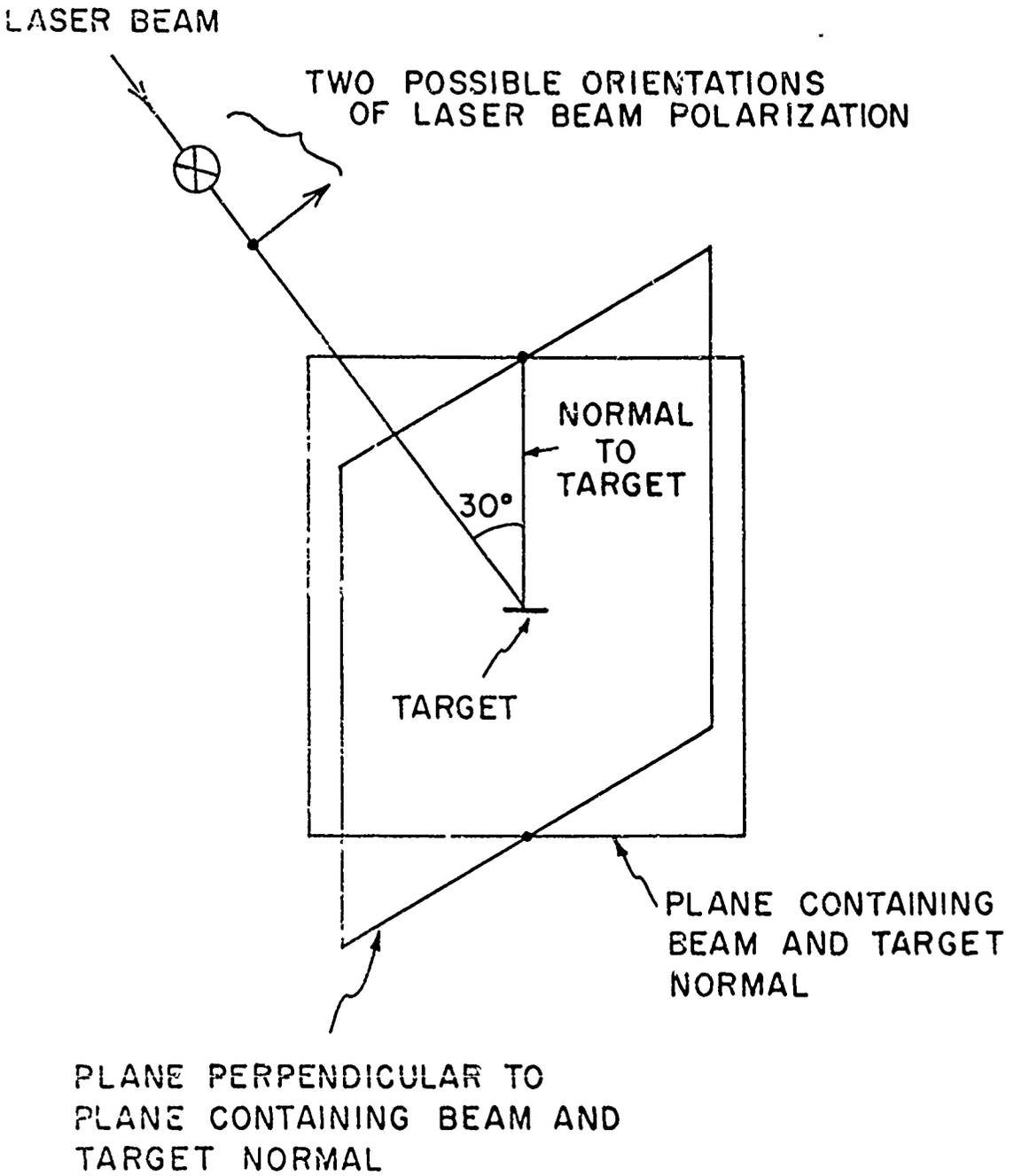

Figure II-4. Geometrical Arrangement for Measurement of Angular Distribution, Showing Orientations of Laser Polarization and of Planes in which the Distribution was Measured.

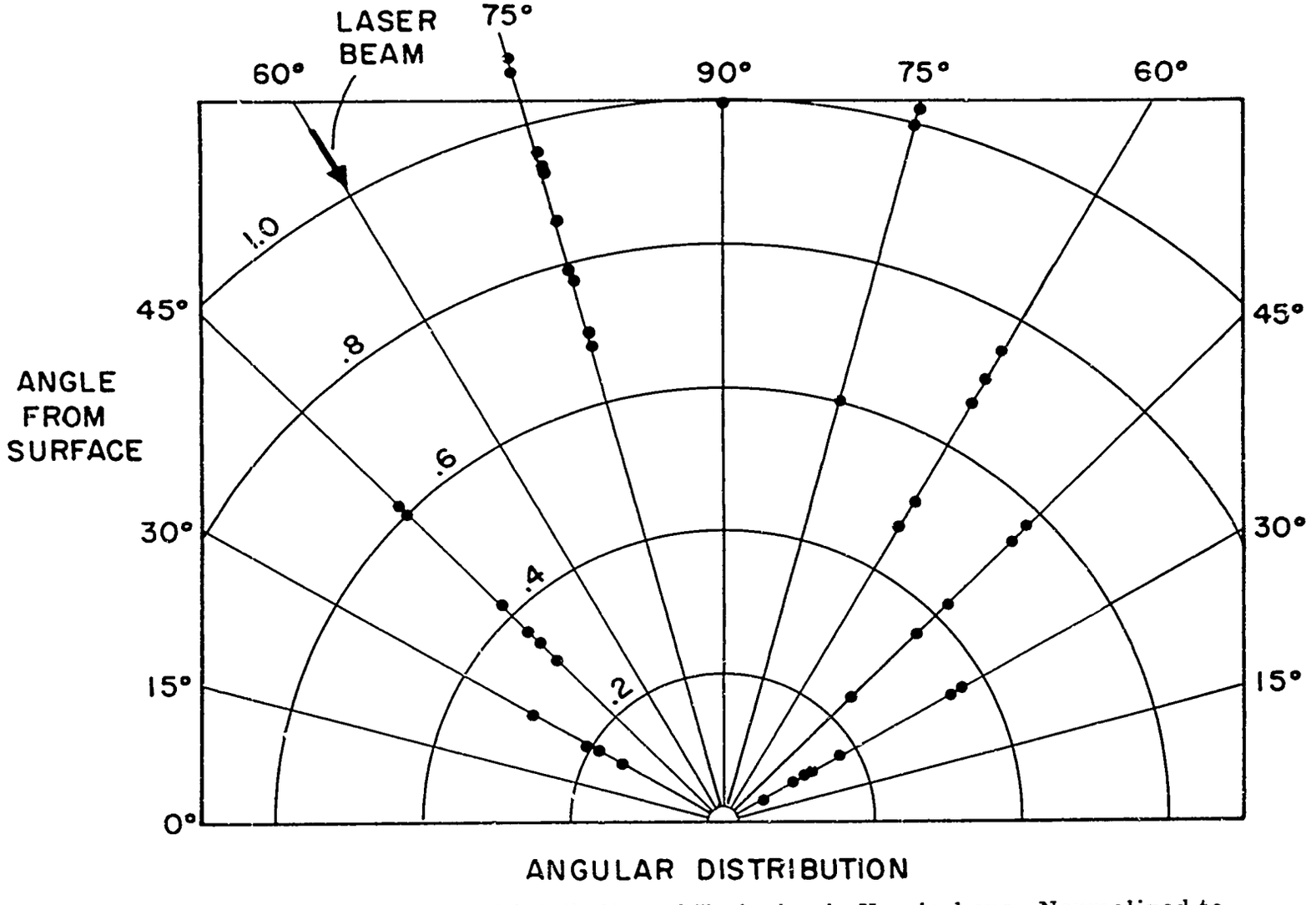

Figure II-5. Angular Distribution of Emission in Hemisphere, Normalized to Unity at 90° to Surface of Target. Data are for Measurements with the Laser Beam in the Plane of the Detectors and with the Polarization Perpendicular to the Plane Containing the Laser Beam and the Target Normal.

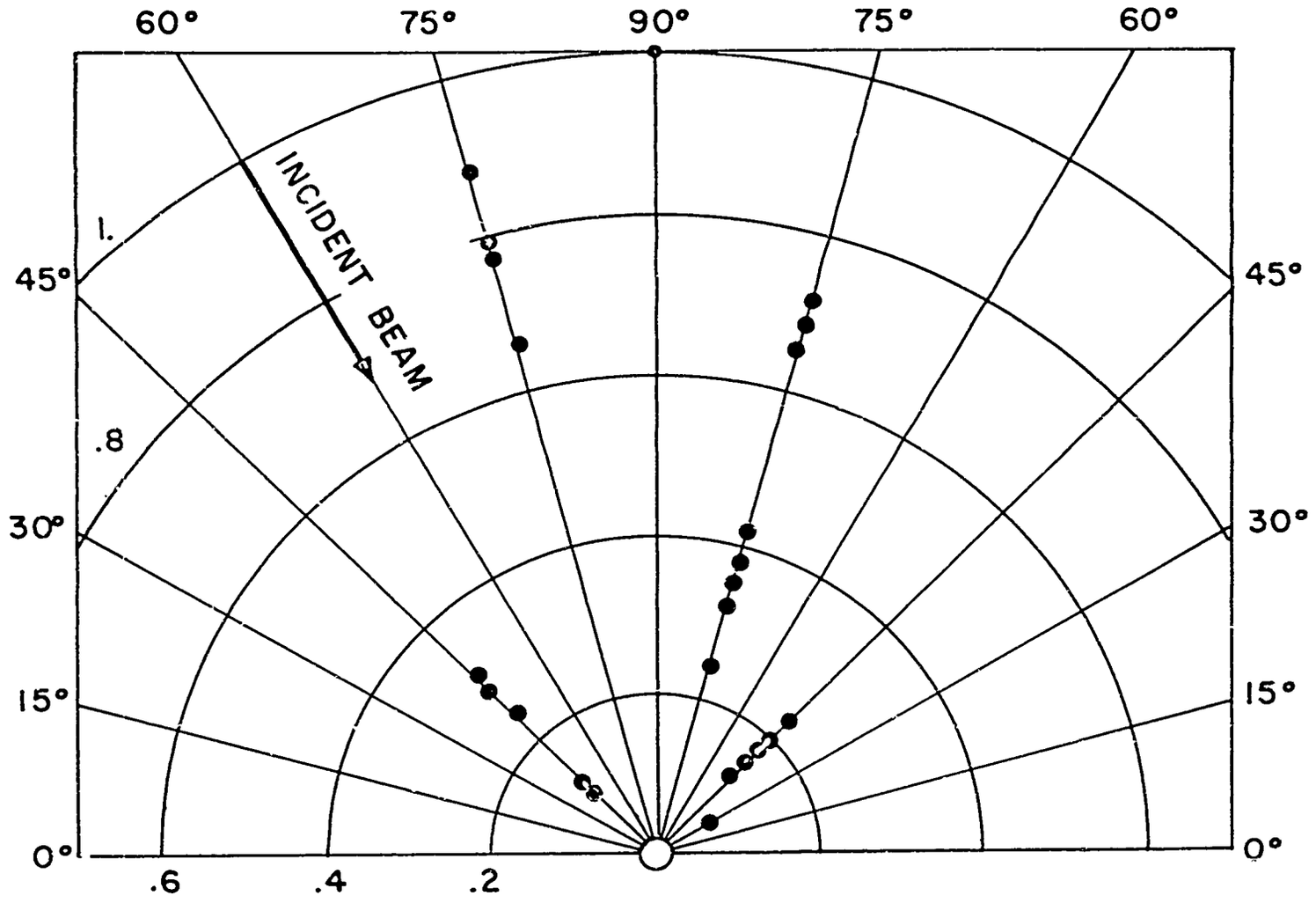

Figure II-6. Angular Distribution of Emission in Hemisphere, Normalized to Unity at 90° to Surface of Target. Data are for Measurements with the Laser Beam in the Plane of the Detectors and with the Polarization in the Plane Containing the Laser Beam and the Target Normal.

as in that figure but the direction of the polarization of the laser beam was perpendicular. There is little difference in the results. Thus, the relative orientation of the polarization does not appear to affect the angular distribution of the emission.

3. Multiplier Detector

As part of the effort to study and interpret the different phenomena occurring in the chamber, in particular to elucidate the possible role of emission of secondary electrons from the collector surfaces in producing the observed signals, we replaced the collector along the normal to the target surface with a multiplier detector. This detector has a beryllium-copper cathode and a series of dynodes which amplify the electron emission from the cathode. This is the same type of detector used on the time-of-flight spectrometer. In the original collector arrangement, a high energy ion striking the surface of the collector could cause secondary emission of an electron. If this electron escapes from the surface, it affects the output signal, corresponding to a movement of charge in the same direction as the collection of ion current. Thus, even if a neutral plasma moved across the gap and struck the collector surface, there could still be a net signal indicating arrival of positive charge.

In order to add the multiplier to the system, an auxillary flange was machined so that the cathode of the multiplier is farther removed from the target than the original collector position. Some data obtained with this arrangement are shown in Figure II-7. The upper trace is the signal from the multiplier; the lower trace is the signal from a collector located at an angle of 15° from the normal to the target surface. The ratio of the time of arrival of the last peak on the multiplier trace and time of arrival of the main peak in the lower trace is equal to the ratio of the distances from the target to the multiplier cathode and from the target to the collector. This

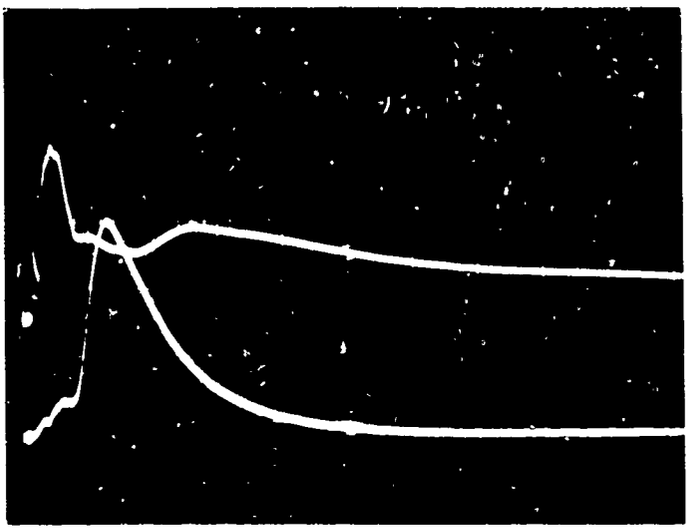

Figure II-7. Signal from Multiplier. Top Trace is Multiplier Output, 0.2 V/cm. Bottom Trace is Output from Collector at 15° to Target Normal, 0.005 V/cm. Sweep Speed: 5μs/cm.

suggests that these two peaks are due to arrival of the same group of particles. The first peak on the upper trace, which is visible only as it returns to the base line, is presumably due to arrival of ultraviolet radiation. The entire upper trace is similar to the high energy neutral molecule pulses obtained on the quadrupole spectrometer. The results indicate that secondary emission does play a role in the relative sizes of the signals. In particular, it indicates that part of the observed signals may be due to passage of neutral molecules which produce secondary electron emission.

The high peak in the upper trace apparently corresponds to one of the smaller pulses in the lower trace before the main peak. This could suggest that the sensitivity of emission of various material surfaces is different for different types of particles. In an attempt to obtain data on this point, a collector with a beryllium-copper surface was installed. (The original collectors are stainless steel.) The output of this collector was identical in shape to the output of the stainless steel collectors, differing by a multiplicative factor of the order of unity. This indicates that the difference in pulse shapes between the multiplier and ordinary collectors does not originate in different secondary emission coefficients for different materials.

It appears that the most likely explanation of the different shapes of the two curves in Figure II-7 is that the multiplier responds to secondary emission processes at the cathode, but not necessarily to direct collection of charged particles reaching the cathode. Secondary electron emission is important in affecting the shapes of the observed signals. Neutral hydrogen desorption, for example, may be easily seen by the multiplier but not detected as more than a small break in the trace of a collector without extra amplification.

Additional data from the multiplier indicates that applying a voltage to the target while keeping the hemisphere grounded had no effect on the signal. However, when the target was grounded and voltage was applied to the hemisphere, noise was present in the multiplier output so that no good data were obtainable. It was apparent that application of an accelerating voltage for ions did not affect the transit time of the pulse observed on the multiplier, however.

These results indicate that the collector signals arise from a mixture of direct ion collection and secondary emission by both neutral molecules and ions. The angular distributions reported before are therefore for this mixture, rather than only for ions. Since the multiplier responds only to secondar emission. its pulse shape may well be different. We shall return to this point later in the section on analysis.

4. Bipolar Collector

We also took data with a bipolar collector in place of one of the usual collectors. The bipolar collector was inserted in place of a collector at 15° from the normal to the target surface. The design is similar to that described by Haught.[7] We obtained a signal which begins approximately five microseconds after the laser pulse and which represents the integrated amount of charge that has arrived. A typical oscilloscope display is shown in Figure II-8. The electron collection is much larger than the positive ion collection.

In the usual collector measurements we see positive signals. This would lead to an expectation of a positive charge collection at least as great as the negative charge collection. If a neutral plasma travels from target to collector, the charge collections should be equal for both signs of charge.

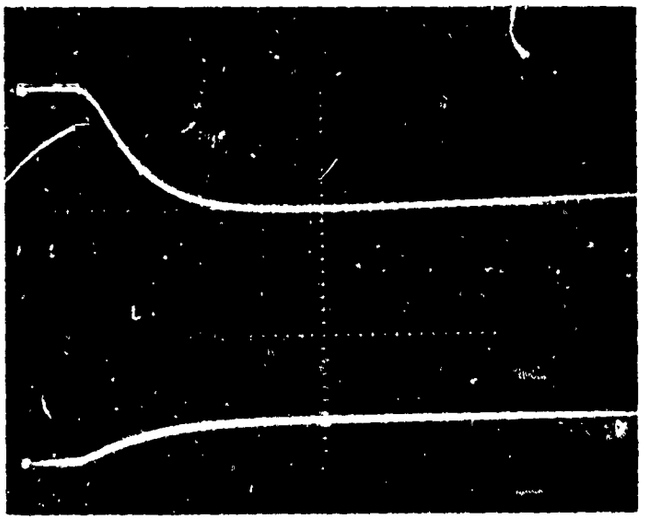

Figure II-8. Output of Bipolar Collector. Upper Trace Electron Collection, 200 V/cm. Lower Trace: Ion Collection, 5 V/cm. Sweep Speed: 5μs/cm.

Some difference between the signals caused by the two different signs of charge at the bipolar collector would be expected on the basis of the secondary electron emission produced by ions striking their collecting electrode. However, this difference should not be larger than a factor of two and the observed difference is much larger.

We investigated the possibility that because the ion mobility is lower than the electron mobility, the applied electric fields were not high enough to sweep all ions to the collector. This was done by applying larger voltages to the positive charge collection electrode. The results indicate that the positive charge collection was not affected by the magnitude of the voltage applied. However, applying a large voltage to the positive charge collector did suppress the negative charge collection. We interpret this as being evidence that the negative charge collection is largely spurious, and originates in the region of the collector and does not truly represent charge that has traveled from the target. Application of the large negative voltage reduces the region in which the extra electrons can originate and suppresses the amount of negative charge that can be collected. An additional piece of information is that at very low laser powers the magnitudes of the two charge collections become much more nearly equal. When an anomolously small laser pulse occurs, the magnitude of the electron collection decreases much more than the amount of the positive ion collection. Haught[7] observed a similar effect of larger electron currents than ion currents, and also attributed it to spurious electron collection. He had the advantage of being able to know the total number of electrons in his small sample, so that if the collected number exceeded this number, it was definite proof that additional charge was being produced in the region of the collector.

The signals observed on the bipolar collector generally increase with increasing laser flux density. In fact, at large signals, the electron collection saturates so that the voltage drop is approximately equal to the externally applied voltage. It is apparent that a larger signal could not be obtained. If the electron collecting voltage is increased, the saturation voltage is also increased.

An investigation of the effect of applying a voltage to the target showed that target voltage did not affect the signal received at the bipolar collectors. This is in agreement with the results obtained with the ordinary collectors and we would not expect to see an effect. There is some correlation between the laser pulse size and the signals on the bipolar collector. In general the largest signals occur with the largest laser pulses, and the smallest signals with the smallest laser pulses, but there is much scatter. Also, the signals associated with the largest laser pulses arrive slightly sooner than those with the smaller laser pulses. The total charge collection corresponds to about 2×10^{12} negative charges and 10^{10}-10^{11} positive charges. (This is for one bipolar collector; the total emission of ions thus would be of the order of 10^{13} or 10^{14} when the solid angle and anisotropy of emission are considered.)

Since the detector circuitry is an integrating circuit, the derivative of the observed pulse shapes should be the same as the pulse shape observed on the ordinary collectors. This is the case, as we see in Figure II-9 which shows that the charge collection does indeed correspond to the signals observed on the other collectors.

In an attempt to investigate the structure of the field around the bipolar collector, we modeled the electrode configuration on conducting paper as described in the last semi-annual report.[6] This method involves plotting equipotential surfaces on a sheet of conducting paper in which the

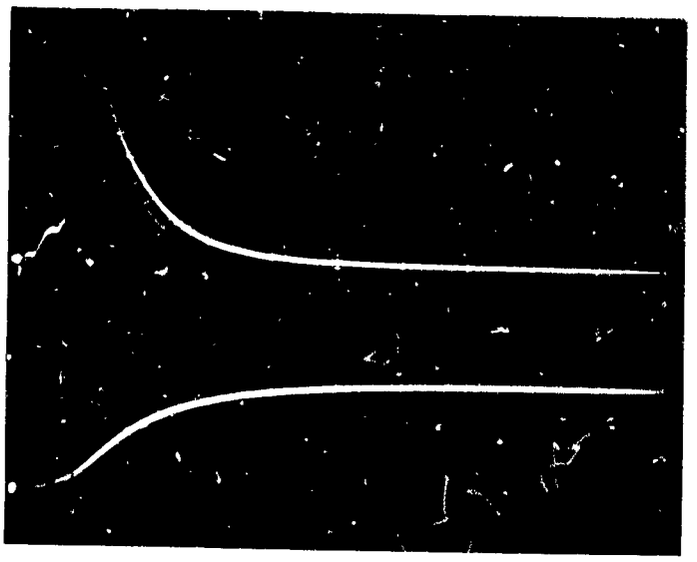

Figure II-9. Comparison of Bipolar and Ordinary Collectors. Upper Trace: Signal from Collector at 15° to Target Normal, 0.01 V/cm. Lower Trace: Ion Collection at Bipolar Collector, 2 V/cm. Sweep Speed: 5μs/cm.

electrode configurations are drawn with silver paste. Appropriate voltages are applied to different electrodes. One of the two terminals of a high impedance probe is tied to a point while the other terminal is moved in the region between the electrodes. The equipotential lines are obtained by following the lines along which nulls occur. Such equipotential surfaces obtained near the region of the entrance to the bipolar collector are plotted in Figure II-10.

This investigation was undertaken to see if possible distortion of the field or fringing of the field through the shielding wire grid could lead to the difference in the positive and negative charge collection. As Figure II-10 shows, the grid is a good shield, with little penetration of the applied field through it, and within the bipolar collector the field distribution is approximately symmetric. Although the complete three dimensional structure is not modeled, we feel that a good qualitative picture is obtained. Thus, there is no asymmetry or fringing to explain the difference in charge collection. This result substantiates our earlier assumption that the grids across the holes in the hemisphere do provide field continuity and good shielding for charged particles passing from the target to the region of the hemisphere.

We compared the charge collection on the ion half of the bipolar collector to the area under the current vs time curve from an ordinary collector. The bipolar collector should represent the true ion collection, since it is not in a line of sight path with the target. Thus, the signal is all produced by particles which are brought to it by the applied field. (The signal may be increased slightly by secondary emission, but it should represent approximately all the ions arriving at the collector.) The ordinary collector signal is consistently larger by a factor of 2. This result agrees with the results of the multiplier experiment described earlier, in that the total signal at a collector arises from a mixture of direct charge collection and

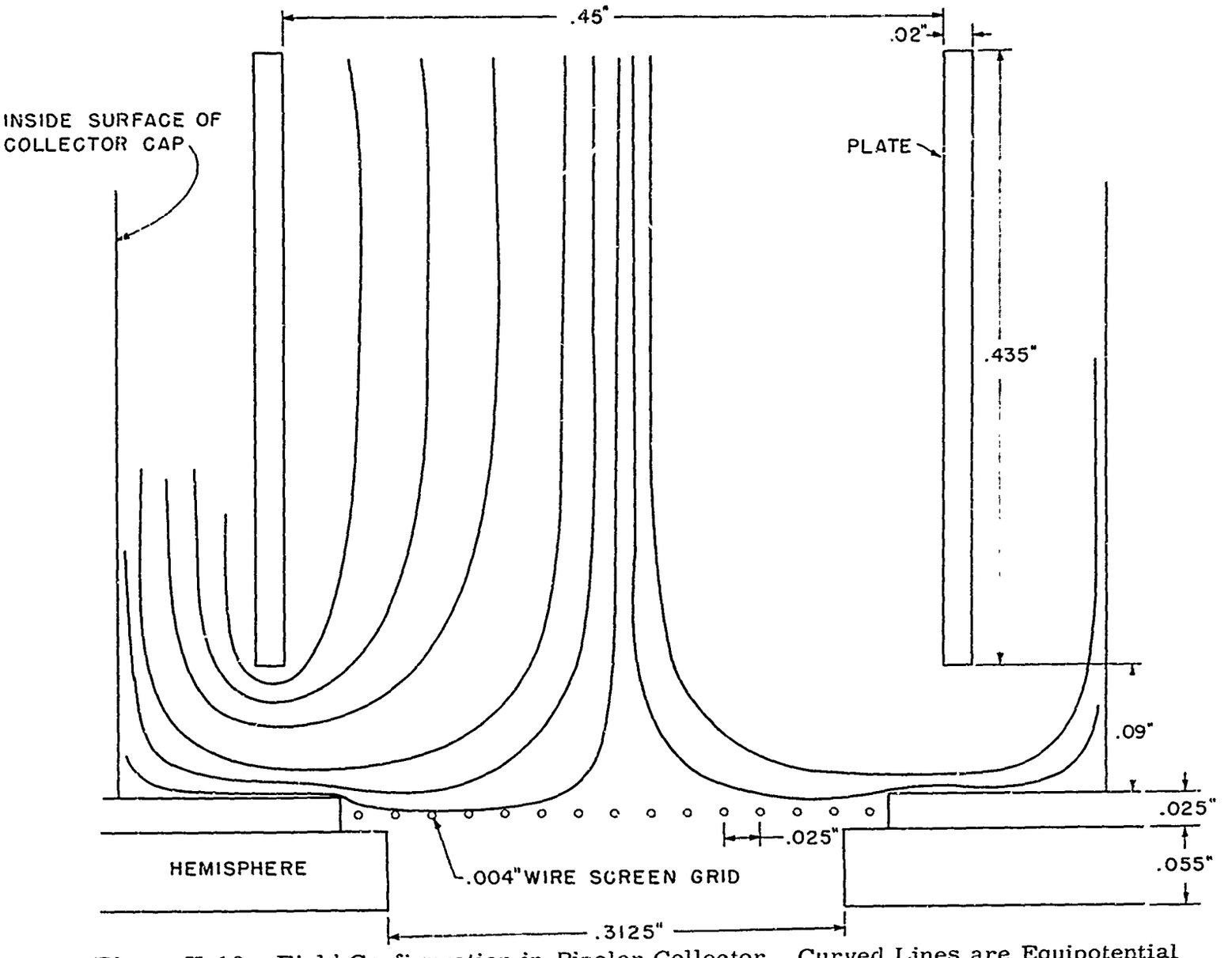

Figure II-10. Field Configuration in Bipolar Collector. Curved Lines are Equipotential Lines. Not all Lines are Shown but Distribution is Symmetric on Left and Right Sides.

secondary emission produced by neutral molecules and by ions. It also explains the failure of the collector signal to go to zero with positive voltage applied to the grid.[6] (This is not a problem in the time-of-flight spectrometer since ions would be separated from neutrals by the time the retarding voltage is applied.)

5. Measurements on Ordinary Collectors

As we described in the last semi-annual report,[6] there are a number of puzzling features associated with the voltage pulses observed at collectors and at the hemisphere in the hemispherical interaction chamber. In particular, the effect of applying a voltage to the target gives results which do not appear to be a simple passage of ions. A voltage applied to the target results in a large increase in the signal observed at the hemisphere. This signal occurs at a time coincident with the signal on the collector along the normal to the target surface. (See Figure II-11. This figure is identical to Figure II-4 of the last semi-annual report; it is reproduced here to make the present report self-contained.) The arrival time of the pulses is not affected by the magnitude of the applied voltage. With applied voltage, the ratio of the signals observed at the collector and the hemisphere was approximately equal to the ratio of the solid angles subtended by the collector and hemisphere, especially if the nonisotropic angular dependence of the emission is considered. However, when no voltage is applied, the total charge collection at the hemisphere is somewhat smaller than the charge received at a collector, in spite of the fact that the solid angle subtended by the collector at the target is very small compared to that of the hemisphere. To sum up, with no applied voltage, the pulse shapes were as expected, but the relative amplitudes of these signals were not as expected. On the other hand, with voltage applied to the target, the relative amplitudes are as expected, but the shape of the pulse from the hemisphere does not show the expected

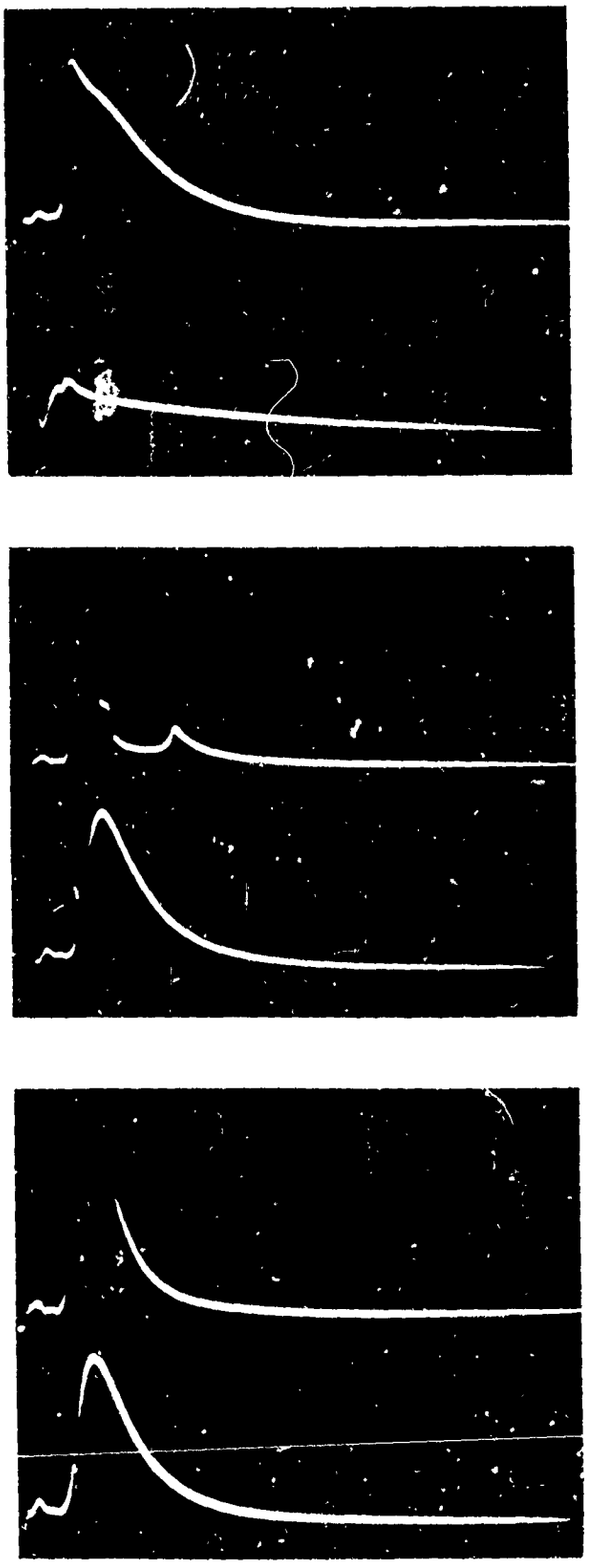

Figure II-11. Effect of Potential Applied to Target. Sweep Speed: 5μs/cm. Upper Traces from Collector Along Normal to Target. Bottom Traces from Hemisphere. All Upper Traces are 0.1 V/cm. In the Top Photograph the Bottom Trace is 0.1 V/cm; in the Middle and Bottom Photographs the Lower Traces are 10 V/cm.

displacement current effect. Work has been done to elucidate these phenomena and we now can interpret a number of these features consistently, as we shall describe later.

We applied a positive voltage to the ordinary collectors. The hemisphere and the retarding grid in the collector structure were grounded. Whenever a positive voltage was applied the signal received by the collector was negative, as is shown in Figure II-12. Only a small applied voltage was necessary to produce this effect. The region with one or two volts applied is apparently a transition region and the signals become noisy. When three volts or more are applied, a negative signal is observed; whereas at zero volts and negative voltage applied to the collector, relative to the hemisphere at ground, the familiar positive signal is observed as in the bottom half of Figure II-12.

This result may be understood as follows: A displacement current in the hemisphere induced by the passage of a small net charge induces a small positive voltage on the hemisphere (bottom trace of top photograph in Figure II-11), so that secondary electrons emitted from the collector are attracted away from the collector, leading to observation of the signal in the bottom photograph in Figure II-12. The presence of a voltage on the collector so that the collector is negative with respect to the hemisphere leads to a reversal of the flow of electron current and to the signal in the top photograph in Figure II-12. This result will be considered again later in the discussion of analysis of results in the hemispherical interaction chamber.

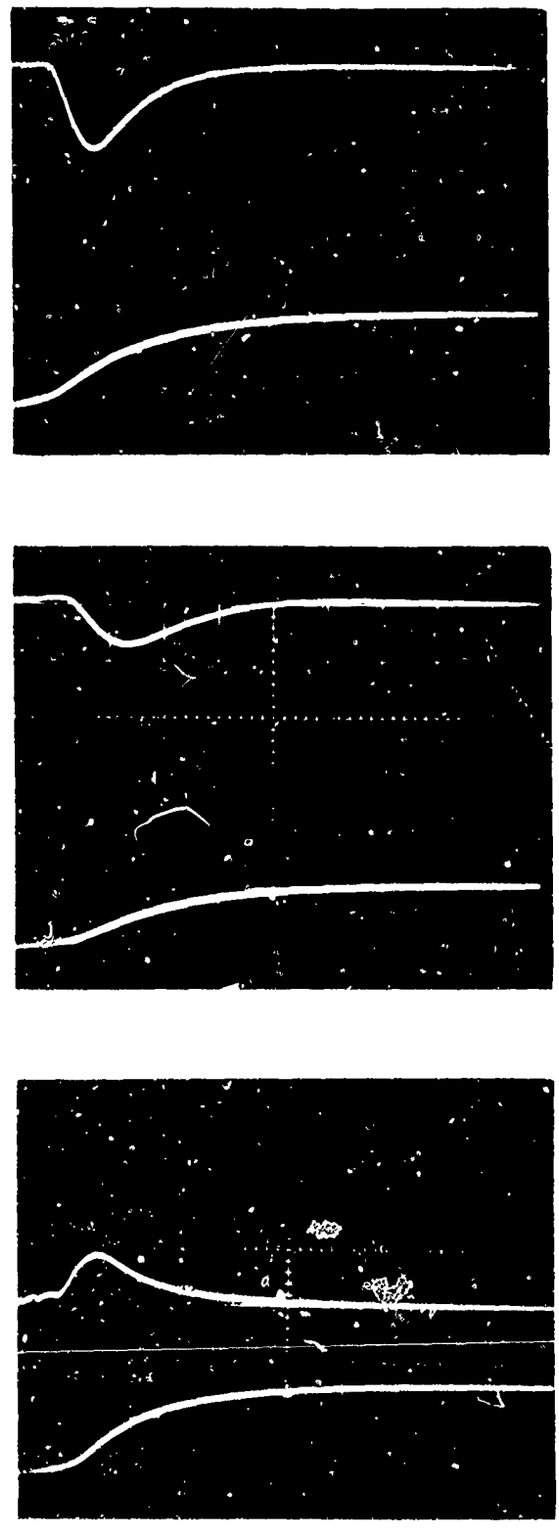

Figure II-12. Effect of Applying Voltage to Collector: Hemisphere and Grid Grounded. Top Traces: 0.01 V/cm, Output of Ordinary Collector. Lower Traces: 0.5 V/cm, Output of ion Collection from Bipolar Collector. Sweep Speed: 5μs/cm. Voltage Applied to Ordinary Collector: (A) +12.5 V, (B) +3.2 V, (C) 0 V.

6. Future Plans

The experiment for measuring the effect of laser flux absorption in the blowoff material in producing high energy ions will be performed according to the setup shown in Figure II-13. A portion of the bottom of the hemisphere will be cut away to allow beam access. Ports are already available in the external chamber so that a beam can be passed transversely across the surface of the target. The experiment will be performed by picking off a portion of the high power laser beam (approximately 100 megawatts) and sending it by means of several reflections from a mirror so that it enters the port at an angle of 30° from the normal to the target surface and is focused on the target surface in the same way as in previous work. The higher power portion of the beam will pass slightly above the target surface and will intercept material emitted from the surface. This system will be difficult to line up, but use of a helium neon laser beam should facilitate the alignment.

B. INTERPRETATION

We shall now consider analysis of the data obtained in the hemispherical interaction chamber. In particular, we shall interpret the various experiments reported above and attempt to consolidate them into a single picture of the operation of the chamber, and also to compare them to earlier results obtained in the time-of-flight spectrometer.[2, 3]

1. Analysis of Hemisphere Pulse Shapes

This subsection gives results of an analysis on the current pulse from the hemisphere when a positive voltage is applied to the target. It had been noted earlier[6] that there are pronounced changes in the signal when a few volts are applied to the target, but when higher voltages were applied,

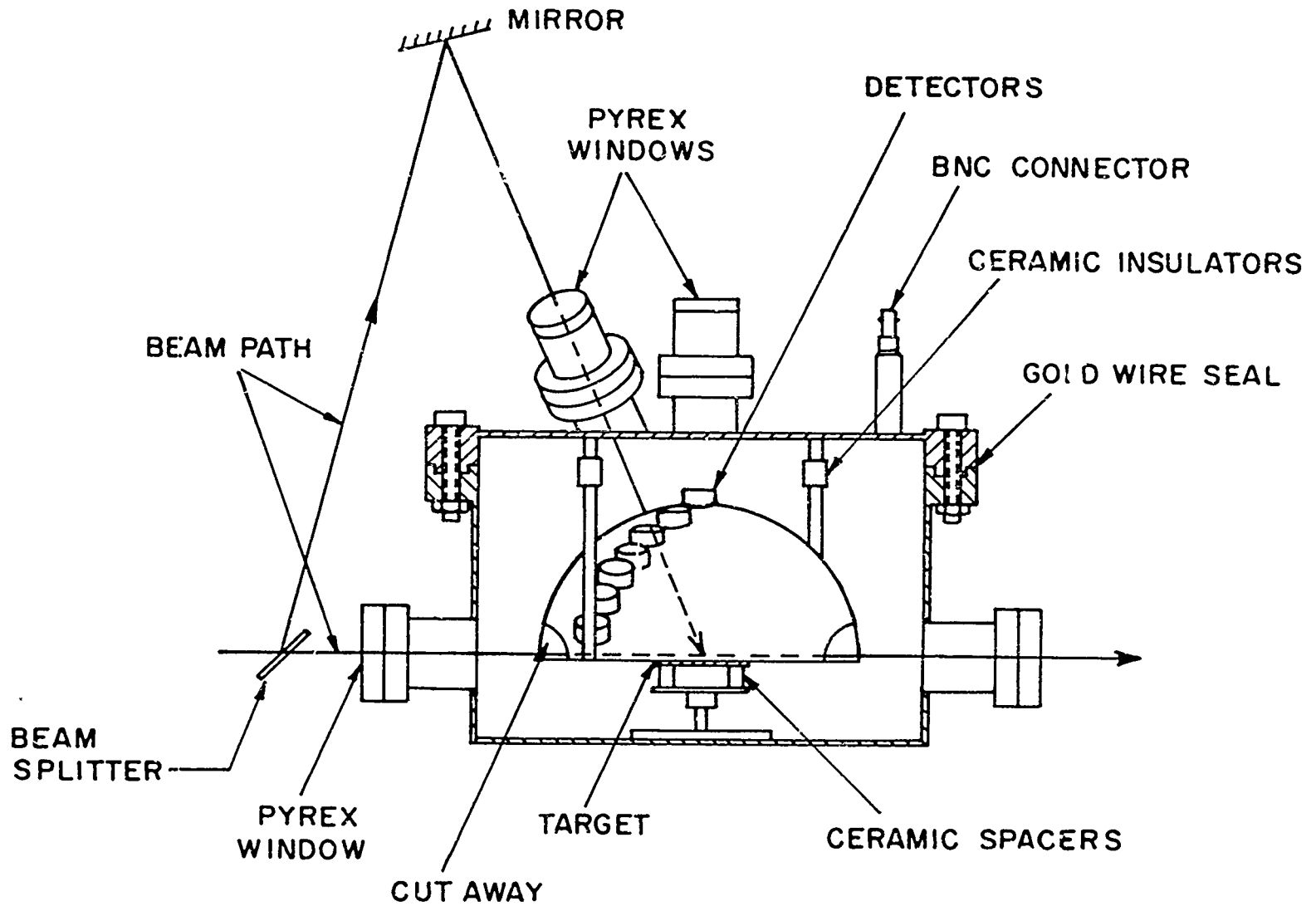

Figure II-13. Arrangement for Experiment with Simultaneous Production of Blowoff Material and Irradiation of Blowoff Material by Laser Radiation which Does Not Strike the Target.

the signal from the hemisphere remained relatively unchanged from what it was with a few volts applied.

This suggests that perhaps the blowoff material traverses the distance from the target to the hemisphere in a neutral state, (possibly as a neutral plasma) and that the heavy particles eject secondary electrons from the hemisphere. The secondary electrons then are accelerated to the target and produce the observed signal. The analysis in this section is done on the basis of that hypothesis.

Under the secondary electron hypothesis, the hemisphere signal at any time should closely represent the rate of arrival of the blowoff material at the hemisphere since the secondary electron transit time should be of the order of 10^{-8} seconds.

Thirty-one photographs were selected from the data taken between May 24, 1967, and August 25, 1967. The criteria used in selection of the oscilloscope traces were

1) A clear signal from both hemisphere and laser monitor.
2) A maximum of 6 photographs for each target voltage.
3) Data for each target voltage should be taken from different dates if possible to ensure a representative sample.

For each set of data the area under the hemisphere signal was measured to indicate the total number of secondary electrons produced. The amplitude of the laser monitor signal was also recorded to indicate laser intensity.

In order to characterize the hemisphere signal by one or two numbers, consider the case where the velocity distribution of the particles in the plasma is given by

$$dN = \frac{4N(v - v_d)^2}{\sqrt{\pi}\, C_o^3} \exp - \frac{(v - v_d)^2}{C_o^2}\, dv \qquad (1)$$

This is a displaced Maxwellian velocity distribution where a drift component v_d is superimposed on a Maxwellian distribution characterized by the thermal velocity $C_o = (kT/M)^{1/2}$

$$v = R/t$$
$$dv = -Rdt/t^2$$
$$v_d = R/t_d$$

where R is the radius of the hemisphere.

$$dN = \frac{4NR^3\left(\frac{1}{t} - \frac{1}{t_d}\right)^2}{\sqrt{\pi}\, C_o^3\, t^2} \exp - \frac{R^2\left(\frac{1}{t} - \frac{1}{t_d}\right)^2}{C_o^2}\, dt \qquad (2)$$

Assuming the yield of secondary electrons is constant with respect to primary particle energy, the observed signal would be proportional to dN/dt. The values of t at the peak and either of the half amplitude points of the signal are designated t_p and t_h respectively.

From the condition that

$$\left\{\frac{d}{dt}\left(\frac{dN}{dt}\right)\right\}_{t = t_p} = 0$$

one obtains the relation

$$\frac{R^2}{C_o^2}\left(\frac{1}{t_p} - \frac{1}{t_d}\right)^2 = 1 + t_p\left(\frac{1}{t_p} - \frac{1}{t_d}\right) \tag{3}$$

From the condition that

$$\left.\frac{dN}{dt}\right|_{t = t_p} = 2\left.\frac{dN}{dt}\right|_{t = t_h} \tag{4}$$

and using equation (3), one obtains the relation

$$\exp\left\{-\frac{R^2}{C_o^2}\left[\left(\frac{1}{t_p} - \frac{1}{t_d}\right)^2 - \left(\frac{1}{t_h} - \frac{1}{t_d}\right)^2\right]\right\} = \frac{2t_p^2\left(\frac{1}{t_h} - \frac{1}{t_d}\right)^2}{t_h^2\left(\frac{1}{t_p} - \frac{1}{t_d}\right)^2} \tag{5}$$

With the measured quantities R, t_p and t_h, the quantities C_o and t_d may be obtained from the simultaneous solution of equations (3) and (5). A computer routine was written to obtain the required solutions.

Suitable roots of the equation were found in only a few of the cases. In these cases the drift component of the velocity was on the average only 20% of the random component. In the other cases a negative drift component was indicated. For the purposes of this analysis it was decided to consider the drift component to be zero. The random velocity component in that case could be obtained from the measurement of t_p using eq. (3) with the $1/t_d$ term neglected.

$$C_o = R/\sqrt{2}\, t_p \tag{6}$$

The fit under these assumptions is shown in Figure II-14 for two of the hemisphere signals. There are two smaller peaks preceding the main peak representing either more energetic particles or ones with lighter mass. While there is no direct identification of the incident particles, it will be assumed (so that we can present the results in the more familiar units of energy) that the particles represented in the main hemisphere peak have the mass of the sodium ion.

The results for the data in the chosen sample are shown in Figure II-15 where the particle energy is plotted against target voltage. There is a scatter of more than a factor of two at the higher target voltage but no definite trend can be seen by examining the points in each of the four time periods. The average random energy (assuming sodium ions) is 11.5 eV.

Figure II-16 shows the number of electronic charges represented by the area under the hemisphere signal as a function of target voltage. While there appears to be a relationship between the number of electrons and the target voltage, closer examination of the data indicates, however, that much of it is associated with variations in laser power. This will be discussed further later.

If the observed hemisphere signal is due to secondary electrons, then an estimate of the total number of incident ions may be made if the coefficient for secondary electrons is known. Unfortunately measurements of the secondary electron yield for low energy alkali ions on stainless steel are not to be found in the literature. Takeishi and Hagstrum[8] investigated the process for the noble gas ions on the refractory metals and on the (111) surface of nickel with ion energies extending down to 4 eV. Coefficients in the range of .03 to 0.2 were observed. Since an Auger process is believed to be involved, the coefficient for the alkali ions could be expected to be somewhat lower.

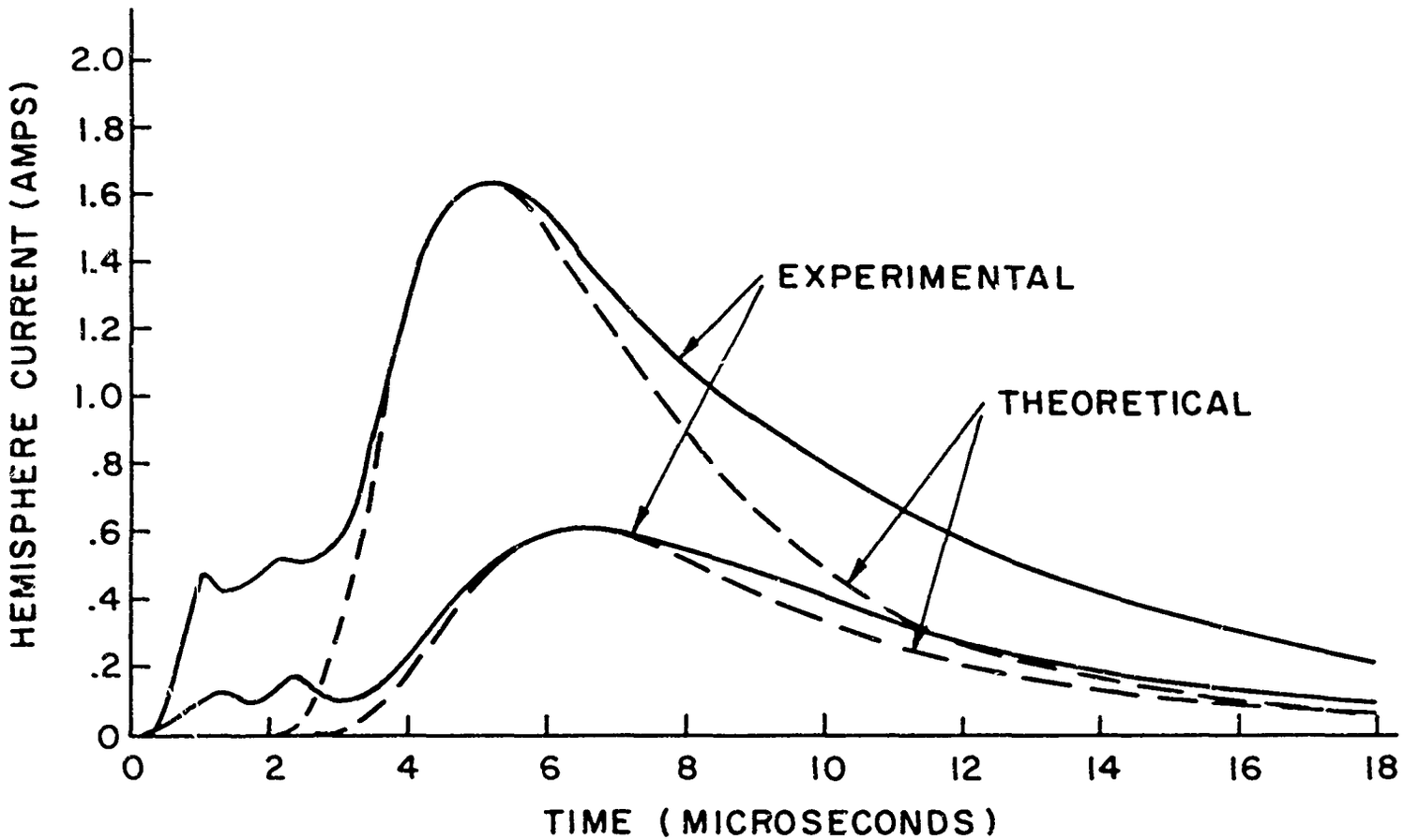

Figure II-14. Two Hemisphere Signals Along with the Fitted Theoretical Curves Assuming a Maxwellian Velocity Distribution for the Primary Particles. Target Voltage was 540 Volts.

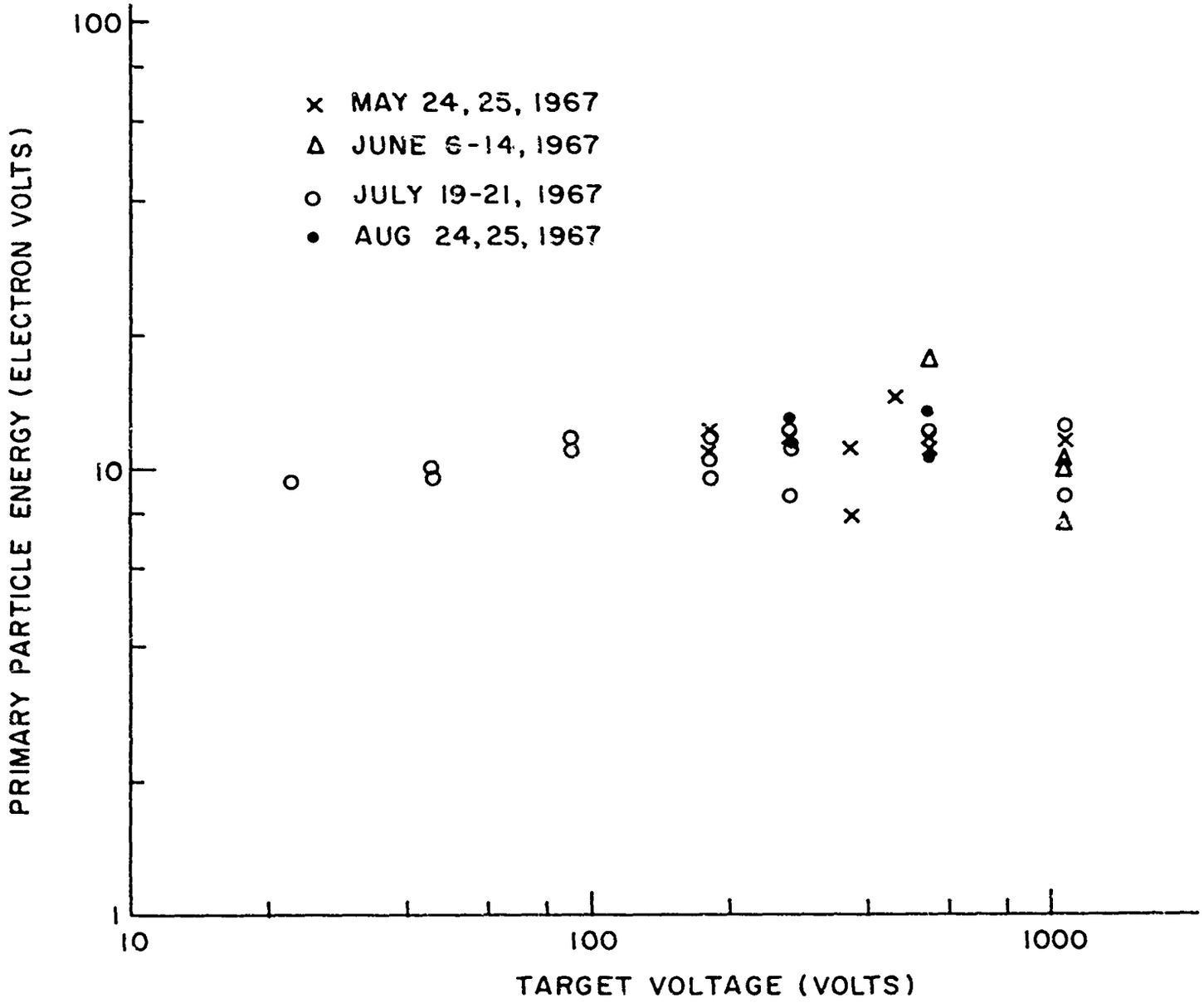

Figure II-15. Primary Particle Energy (Assuming Mass 23) as a Function of Voltage Applied to the Target.

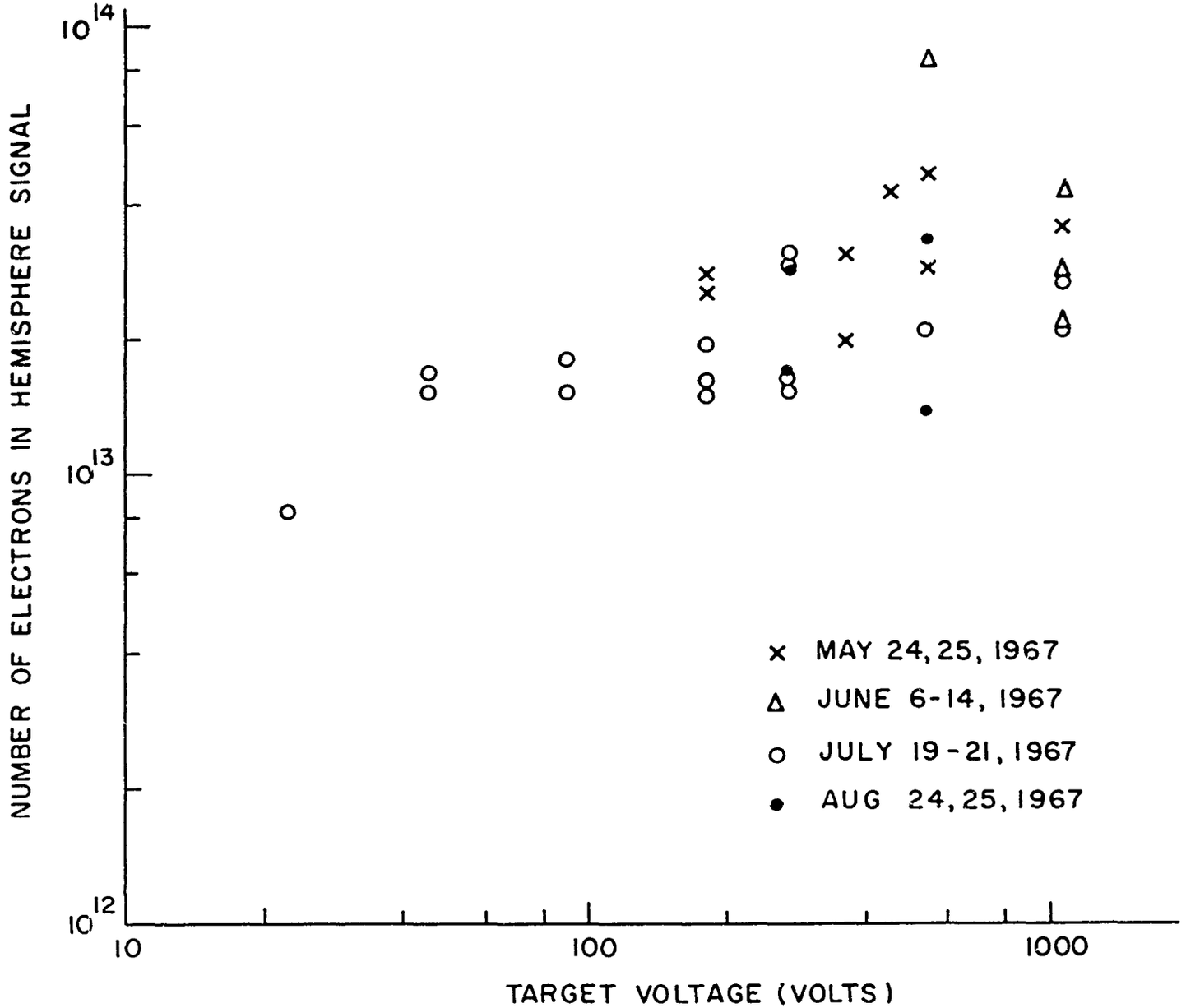

Figure II-16. The Number of Electronic Charges in the Hemisphere Pulse as a Function of the Voltage Applied to the Target.

If we estimate the coefficient for secondary electron emission in the laser experiment at 0.1, then the indication is that in the events represented in the sample the average number of ions produced by the laser interaction is 3×10^{14}.

Examination of the data indicated that some of the variation in the amplitude and shape of the observed hemisphere signal is due to variations in the laser power. For data taker under conditions of calibrated laser power monitoring, a multiple regression analysis was made on the number of electronic charges, N, the target voltage, V, and the laser power P, represented by the amplitude in centimeters of the laser monitor signal. It was found that for a least squares fit

$$N = 1.3 \times 10^{13} V^{0.079} P^{1.027}.$$

Similarly for the incident particle energy, W, the multiple regression analysis showed

$$W = 14 V^{-.0158} P^{0.5302} \text{ electron volts}$$

For this data sample it is clear that variation of the target voltage over more than an order of magnitude has an insignificant effect on either the number of the energy of the incident particles. Variation in the laser power, on the other hand, is found to be significant.

The lack of correlation between the target voltage and the amplitude and shape of the hemisphere signal supports the hypothesis that the blowoff material resulting from the laser interaction travels the distance from target to hemisphere in a charge-neutral stage -- either as a plasma or in molecular form.

The results can be interpreted to mean the laser vaporizes 3×10^{14} particles from the surface and subsequently heats them to an energy of about 10 eV. Such an interpretation requires some comment. This estimate of the number of incident particles is orders of magnitude higher than estimates of the number of ions based on previous experiments.[2, 3] In addition the estimate of energy is lower than for the "high" energy particles previously observed in the time-of-flight spectrometer and higher than for the particles thermally desorbed and observed as a pressure pulse in the quadrupole spectrometer.

Perhaps the first point to be made concerns the identification of the incident particles. The signal from the hemisphere may be due to secondary electrons produced by either ions or atoms or a combination of both. Similarly the signal may be due to sodium, potassium, carbon monoxide, or other species. Comparisons with other techniques must recognize this.

The previous work on high energy ions and molecules must be examined to determine if particles of the nature encountered in the hemisphere experiment were likely to be observed if present.

2. Analysis of Collector Pulse Shapes

We have also analyzed pulse shapes from various collectors in the hemispherical chamber in order to obtain the velocity distribution as a function of angle. The method of analysis is the same as described in our May 1966 report.[3] As expected, the velocity distribution in directions near perpendicular to the target surface peaks at a higher value than the distribution at larger angles. Some results are shown in Figure II-17 for collector No. 7 at an angle of 15° from the normal, and collector No. 10 at an angle of 60° from the normal. The shift of the distribution to higher velocities as the angle from the normal decreases is unmistakable.

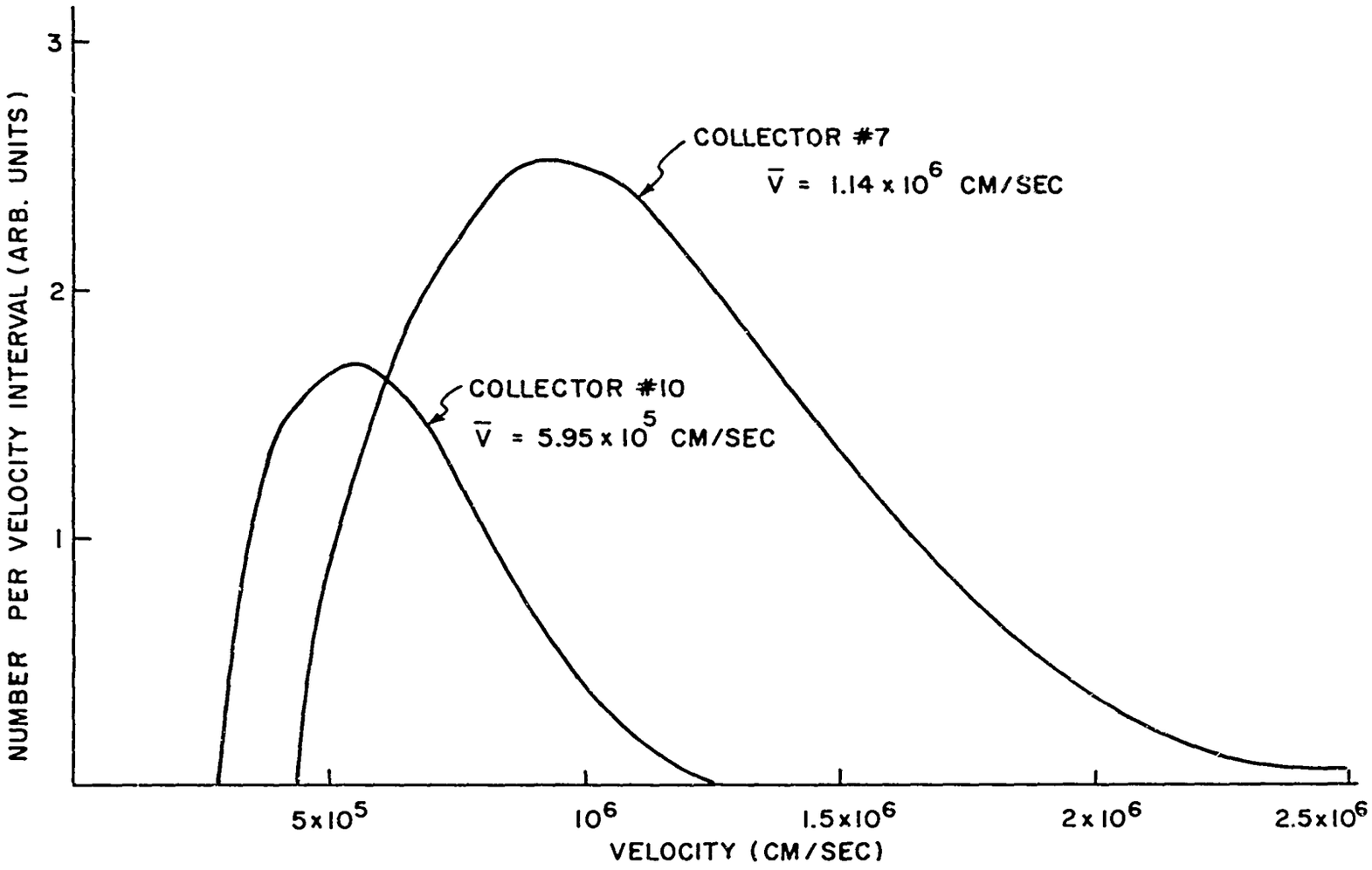

Figure II-17. Velocity Distributions of the Emission as Recorded at Collector #7 at 15° to the Target Normal and Collector #10 at 60° to the Target Normal.

The average velocity of the distribution is shown in Table II-1 for various collectors. Because of the very small signals from collectors at large angles to the surface, there were very few samples that could be adequately analyzed. The energy corresponding to the velocity is of the order of 10 eV, in agreement with the case of the hemisphere signals described above.

When this data is compared to that obtained in the time-of-flight spectrometer, there are a number of differences. (See the May 1966 report.)[3] In the present work, the peak of the distribution normal to the target surface is shifted to lower values. The shape of the pulses is such that the high velocity tail is longer relative to the total shape of the pulse. The reason for the shift of the peak to lower velocities is not understood, although the operating conditions may be somewhat different. The main ion peak (i.e., first large peak to arrive at the multiplier) observed in the time-of-flight spectrometer was due to sodium ions. The tail of the distribution at high velocities in the present curves may be accounted for by a relatively small amount of lower mass ions, since the present system has no mass discrimination. However, the conditions of laser flux density should have been approximately the same in the two different experiments; and if the ion composition is roughly the same as we have assumed previously, the velocity distribution should be similar. It may be that the additional component of heavy ions such as potassium, CO, and CO_2, distorts the curve so that the center of mass of the curves is shifted to a lower value than in the case of a pulse which is known to be made up only of sodium ions. However, the magnitude of the shift is rather large to understand on this basis alone. For sodium, the average velocity corresponds to an energy of about 15 eV (for directions near the normal to the target surface), whereas on the time-of-flight spectrometer, directed energies of the order of 200 eV were observed. The thermal energies do correspond to temperatures of the same order of magnitude as deduced from the time-of-flight spectrometer measurements.

TABLE II-1

ANALYSIS OF COLLECTOR PULSE SHAPES

Collector	Angle from Normal to Target	Average Velocity (cm/sec)
5	15°	10.6×10^5
5	15°	12.5×10^5
7	15°	12.1×10^5
7	15°	11.4×10^5
8	30°	9.5×10^5
8	30°	8.5×10^5
10	60°	6.0×10^5

3. Hemisphere Operation

It is apparent from the comparison of the data from the hemisphere and from the time-of-flight spectrometer that there are large differences, both in the number of charged particles and in their energies. Thus the hemisphere has not provided a complementary instrument to the spectrometer, as we had expected, and further work is required to understand the differences.

We have, however, removed some of the problems associated with operation of the hemisphere and we feel that our understanding of some of the puzzling features[6] of the data from the hemisphere has improved. From the experimental observations described in Section II A, we derive the following interpretation of the operation of the hemisphere. A neutral plasma along with neutral molecules is produced by laser irradiation of the target. The plasma density is large enough that it is not affected significantly by applied fields, so that during expansion of the blowoff material, application of a field between the hemisphere and the target does not appreciably change the transit time of the charged particles. Since the total net charge flowing is small, only small displacement current effects are seen at the hemisphere. When the particles (ions and neutral molecules) strike the hemisphere, they cause secondary electron emission. With no applied voltage, little secondary electron emission escapes from the region of the hemisphere, because as a small current begins to flow, the hemisphere becomes charged positively and electrons are attracted back to the hemisphere.

Also the small displacement current that does flow (bottom trace of top photograph of Figure II-11) means that the hemisphere is slightly positively charged when the particles arrive. The current due to secondary electrons is registered in the external circuit in the same sense as arrival of positive charge. The material that penetrates through the holes in the hemisphere

to the collectors also causes secondary electron emission at the collectors. However, since the hemisphere is at a positive potential relative to the collectors, electrons emitted from the collectors escape from them, so current is observed there.

Application of a voltage on the collector (as in Figure II-12) bears out these results. When the potential is applied (a potential just large enough to counteract the effect of the potential induced on the hemisphere), secondary electrons will not escape from the collector and additional electrons are attracted to the collector so that the direction of current flow from the collector is reversed, as shown in Figure II-12.

When the target is positive with respect to the hemisphere, however, secondary electrons can escape from the hemisphere and flow to the target. Therefore, application of voltage at the target considerably increases the signal observed at the hemisphere (Figure II-11), so that the ratio of the hemisphere and collector signals is the same as the ratio of their solid angles. This explains the absence of large displacement current effects and the absence of a time dependence of the observed signal on the accelerating potential. At the same time the amplitude of the signal from a collector will not be strongly influenced by the applied potential because of shielding by the grid.

The shape of the current pulse at the hemisphere when voltage is applied to the target is thus explained as follows: Ions travel to the hemisphere from the target in the plasma state, along with neutral molecules, so that there is little displacement current. On striking the hemisphere, secondary electrons are ejected which are accelerated back to the target. (In the absence of an applied potential, these electrons would not escape because of the small induced potential attracting them to the hemisphere.) All

emitted secondary electrons produced by particle impact on the hemisphere are collected so that the signal is increased relative to the zero applied voltage case. Since the hemisphere is almost the same distance from the target as the collectors, the time dependence of the two signals will be approximately the same.

The signal from the collectors does not change when voltage is applied to the target. With no applied voltage, the small voltage induced on the hemisphere collects essentially all secondary electrons produced by particle bombardments of the collector. Applying a voltage therefore does not increase the fraction of these secondary electrons that are collected.

The data from the multiplier indicates the presence of neutral molecules and substantiates the role of secondary emission in making a strong contribution to the observed signals from the collectors and the hemisphere.

The data on the ion collection in the bipolar collector probably gives a better indication of the total positive ion production than the data from the ordinary collectors. These values are higher than those obtained using the time-of-flight spectrometer. The applied field within the bipolar collector is large enough to be able to pull apart the plasma and collect all the ions efficiently. The observed ion current may be increased somewhat by secondary emission from the electrode, but this effect should be less than a factor of two. Further, the observed arrival rate of charge at the position of the ion collector should give a true representation of the flow of the heavy particles from the region of the target.

The ordinary collector signal thus arises from two different contributions: direct charge collection and secondary emission produced by both ions and neutral molecules.

The relative fractions of the collector signal arising from these two contributions are not easily determined, because of lack of knowledge of secondary emission coefficients. The fractions may indeed change as a function of laser power, target surface condition, etc. The fact that the ions travel along with electrons in a condition of approximate charge neutrality also makes it difficult to determine the direct charge collection. However, it seems probable that the observed signals arise from a mixture of these causes.

The measurements in the bipolar collector indicate a substantial amount of charge ($\sim 10^{13}$ - 10^{14} ions per laser pulse) but this charge may travel along with electrons so that the net current is small. Only after separation of the two signs of charge in the bipolar collector can we get a good estimate of the total number of ions. The ion signal from the bipolar collector is thus interpreted as the best measure of the total number of ions in the blowoff material.

Although the above picture is consistent in terms of the various types of measurements made on the hemisphere, it does not offer an insight into the differences between hemisphere results and time-of-flight spectrometer data. We do not understand these discrepancies at present and intend to perform further studies on these points. A possible hypothesis is that there exists a small group of high energy ions that escape from the blowoff material and that these are measured in the time-of-flight instrument, but they do not provide a large enough signal to stand out from the larger background of slower ions which travel as a neutral plasma and provide the bulk of the signal observed in the hemisphere.

SECTION III

CARBON DIOXIDE LASER WORK

The carbon dioxide laser has a number of features that make it attractive as a replacement for the Q-switched ruby laser in the investigation of laser surface interactions. The first of these features is the ability to repetitively Q-switch at kilocycle rates with reproducible pulse shapes and power outputs. Second, the mode structure of the output can be easily controlled; thus the beam can be focused to a much smaller spot than the ruby lasers currently being used. Third, even though the peak power output available from a Q-switched CO_2 laser is about three orders of magnitude lower than that obtainable from the ruby lasers used in this work, the absorption cross section for inverse Bremsstrahlung at 10.6 microns is approximately 3600 times larger than at 6943 Å. Hence, the same temperatures should be obtained in a plasma that is irradiated with the output of either a Q-switched carbon dioxide or the Q-switched ruby lasers used in our previous work. This does not mean to imply that the same temperatures can be obtained on a metallic target from a single pulse of the CO_2 laser as are obtained from a single pulse from a Q-switched ruby laser. For metallic targets the main factor controlling the temperature rise is the loss due to conduction. The absorption mechanism is independent of wavelength and the reflection coefficient is much higher at 10.6 microns than it is at 6943 Å; thus, the temperature rise from a single pulse from the CO_2 laser will be much smaller than that from a Q-switched ruby laser.

What we propose to do, at least until higher powers are available from Q-switched CO_2 lasers, is to continously irradiate the surface under study with the output of a CW carbon dioxide laser and to repetitively Q-switch another laser onto the material that evaporates from the target. By using this technique we will be able to monitor the temperature of the plasma

produced by the continuous laser beam using optical spectroscopy. We will also be able to examine the change in the relative intensities of the emission lines from different states of ionization as the second laser is Q-switched onto the plasma and from that infer the effect of inverse Bremsstrahlung on the heating of the plasma.

The advantages that we expect to realize by using a carbon dioxide laser instead of a Q-switched ruby laser are that we will be able to make more accurate measurements due to the repeatability of the pulse shapes and powers from the Q-switched CO_2 laser, as well as the much high repetition rates attainable. Also, the use of optical spectroscopy as a probe of the plasma temperature should give us much better information of the dynamics of the heating of the plasma while it is happening.

A. LASER CHARACTERISTICS

The carbon dioxide laser being used for the laser-surface interaction measurements consists of a 50 cm long water-cooled tube with Brewster angle sodium chloride windows at either end. The cavity is formed by a long radius mirror configuration consisting of a 3m radius quartz substrate with gold evaporated on it and a flat output mirror made of Irtran-2 with an 85% reflecting dielectric coating on the inner surface and antireflection coating on the outer surface. A mixture of carbon dioxide, nitrogen, and helium flows in at the two ends of the tube and is pumped out from an exhaust port at the center of the tube; this flow configuration prevents small particles that may be borne in the stream from adhering to the windows and causing them to cleave when they are heated by the radiation from the laser. The discharge is fed by a DC power supply capable of delivering 10 kilovolts at 50 milliamps. A maximum power output of 22 watts in several transverse modes is obtained with the discharge operating at a pressure of 21 Torr, with a flow rate of 0.96 cubic feet/hr of nitrogen, 0.35 cubic feet/hr CO_2, and 3.3 cubic feet/hr helium. Insertion of a one quarter inch diameter aperture in the cavity

near the spherical mirror causes the laser to operate in the lowest order TEM_{00} mode with a maximum output of 18 watts.

The output of the laser is monitored using a Coherent Radiation Laboratories Model 201 Power Meter. The output is concentrated in a number of vibrational-rotational transitions centered at 10.6 microns. The output beam can be focused to spots as small as 0.1 millimeter in diameter by use of a five centimeter focal length lens made of Irtran-2 material. The diameter of the focused beam was determined by putting a piece of anodized aluminum at the focal point of the lens and measuring the width of a line burned on the anodizing.

B. CALCULATION OF THERMAL EQUILIBRIUM PROPERTIES

A calculation of the equilibrium populations of the excited states of several atoms was made to determine the feasibility of producing enough thermal excitation at the temperature obtainable by irradiation of solid targets with the CO_2 laser. These results were required to decide whether or not one could make meaningful spectroscopic measurements of the neutral emission for the purpose of measuring temperature. The populations were determined from the expression [9]

$$N_m = \frac{g_m \exp(-E_m/kT)}{z(T)}$$

where N_m, g_m, and E_m are the equilibrium population, statistical weight, and energy of the mth level respectively. $z(T) = \sum_m g_m \exp(-E_m/kT)$ = partition function of the atom.

The calculations were made using the energy levels given in the tables of Moore.[10] No corrections were made for the lowering of the ionization potential due to Debye screening because the populations of high-lying excited

states are negligible at the temperatures under consideration. Figure III-1 shows the populations of the first resonance levels of the alkali metals as a function of temperature. They were calculated taking into account the temperature dependence of the partition function for the neutral atom. The populations are given as a fraction of the total number of neutral atoms. Thus, in determining the absolute numbers of atoms in each level one must take into account the fact that the total number of neutrals will decrease as the gas becomes ionized. The results for sodium will be used to make an estimate of the amount of power radiated into the sodium D lines by the evaporating sodium atoms from a soda lime glass. The alkali metals were chosen for the above calculation because they represented the majority of the high energy ions in our previous experiments; they are also known to have strong resonance lines suitable for spectroscopic measurements. However, further considerations in section III-C indicate that the alkaline earth metals, of which barium has the lowest ionization potential, may be better choices for spectroscopic studies.

The temperature dependence of the partition function for the first and second stages of ionization of barium, as well as the degree of ionization, have been calculated in order to use these for future estimates of radiated power from lines of singly ionized barium. The calculation of the degree of ionization has been made neglecting the second and higher ionization stages. The neglect of the higher ionization stages will not be justified at high temperatures, but for the purposes of estimating ionization upon CW excitation with the CO_2 laser the results obtained in this manner are sufficiently accurate. Figure III-2 shows the partition function for neutral and singly ionized barium. Figure III-3 shows the population of the first stage of ionization of barium as a function of temperature for three different values of the total density of barium atoms. From it, it is obvious that an appreciable amount of ionization will occur at temperatures of the order of 3000°K. Such temperatures will probably not be obtained under continuous excitation of the target by the CO_2 laser, but they will certainly be obtainable under Q-switching of the CO_2 laser onto the plasma. Thus, it is not unreasonable to expect to observe some of the lines from singly ionized atoms in experiments involving Q-switched excitation of solid targets containing barium with the CO_2 laser.

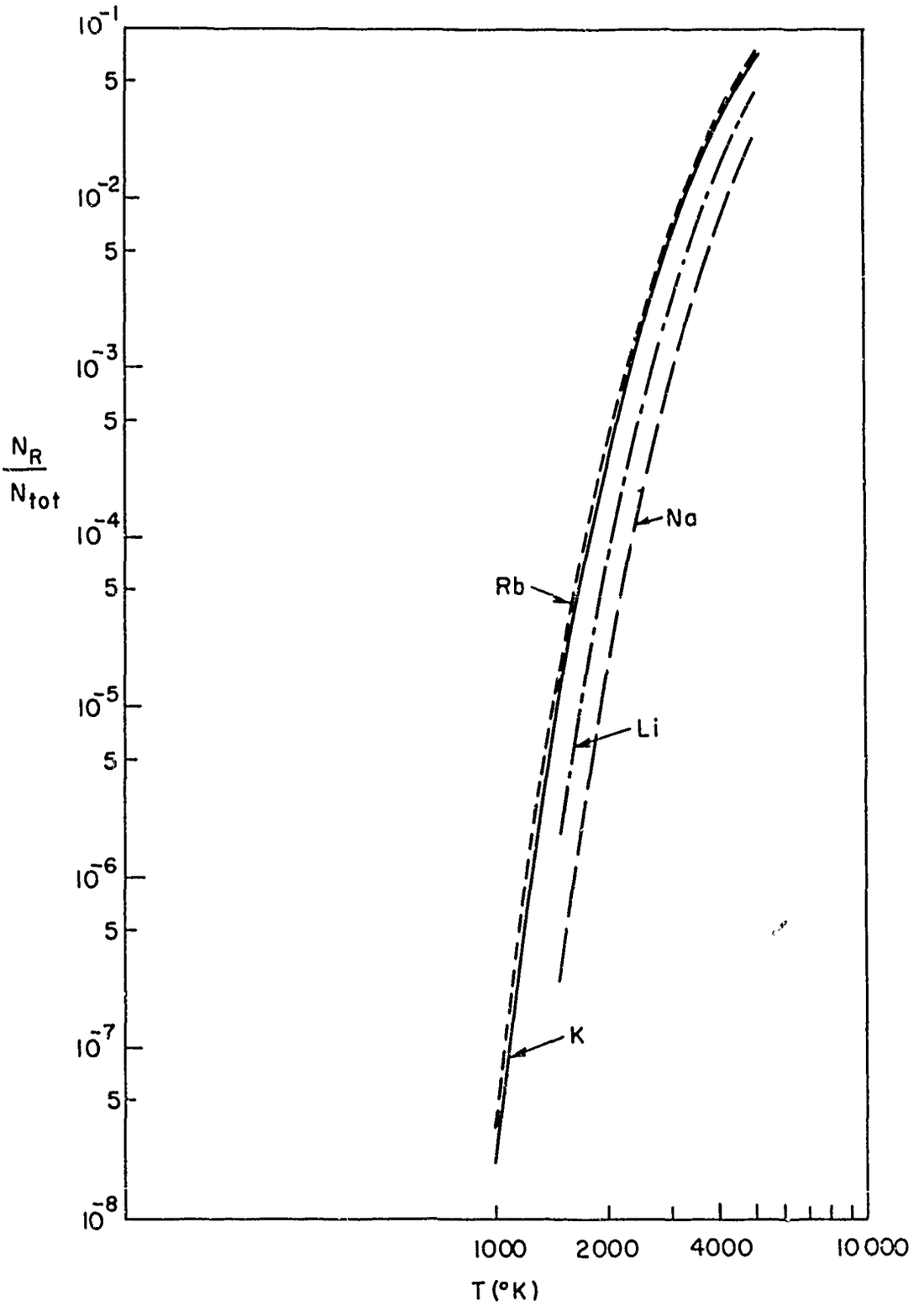

Figure III-1. Fractional Population N_R of First Resonance Levels of Alkali Metals as a Function of Temperature. Curves Represent Combined Populations of $^2P^0$ Doublet.

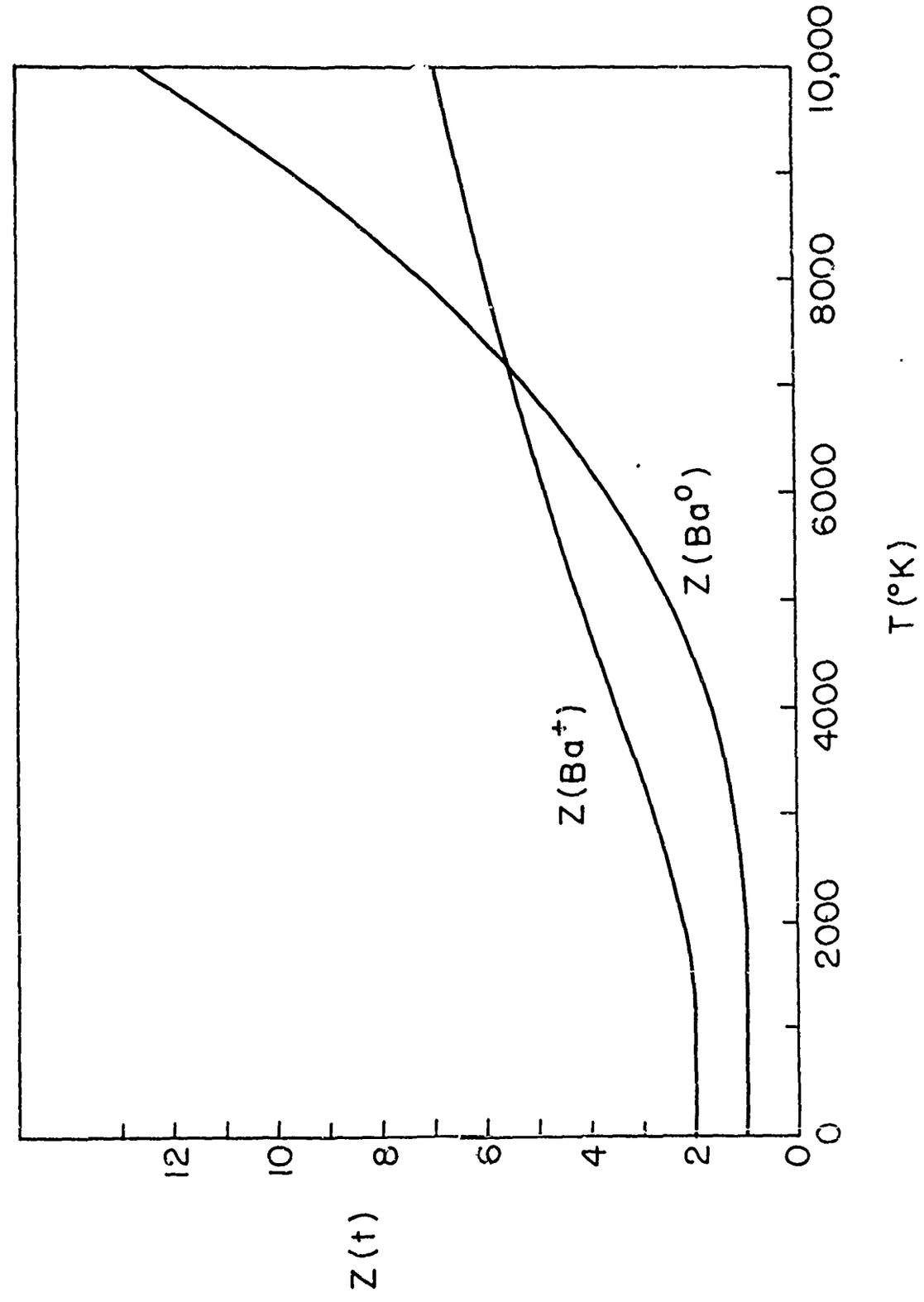

Figure III-2. Partition Functions Z(T) of Neutral and Singly Ionized Barium.

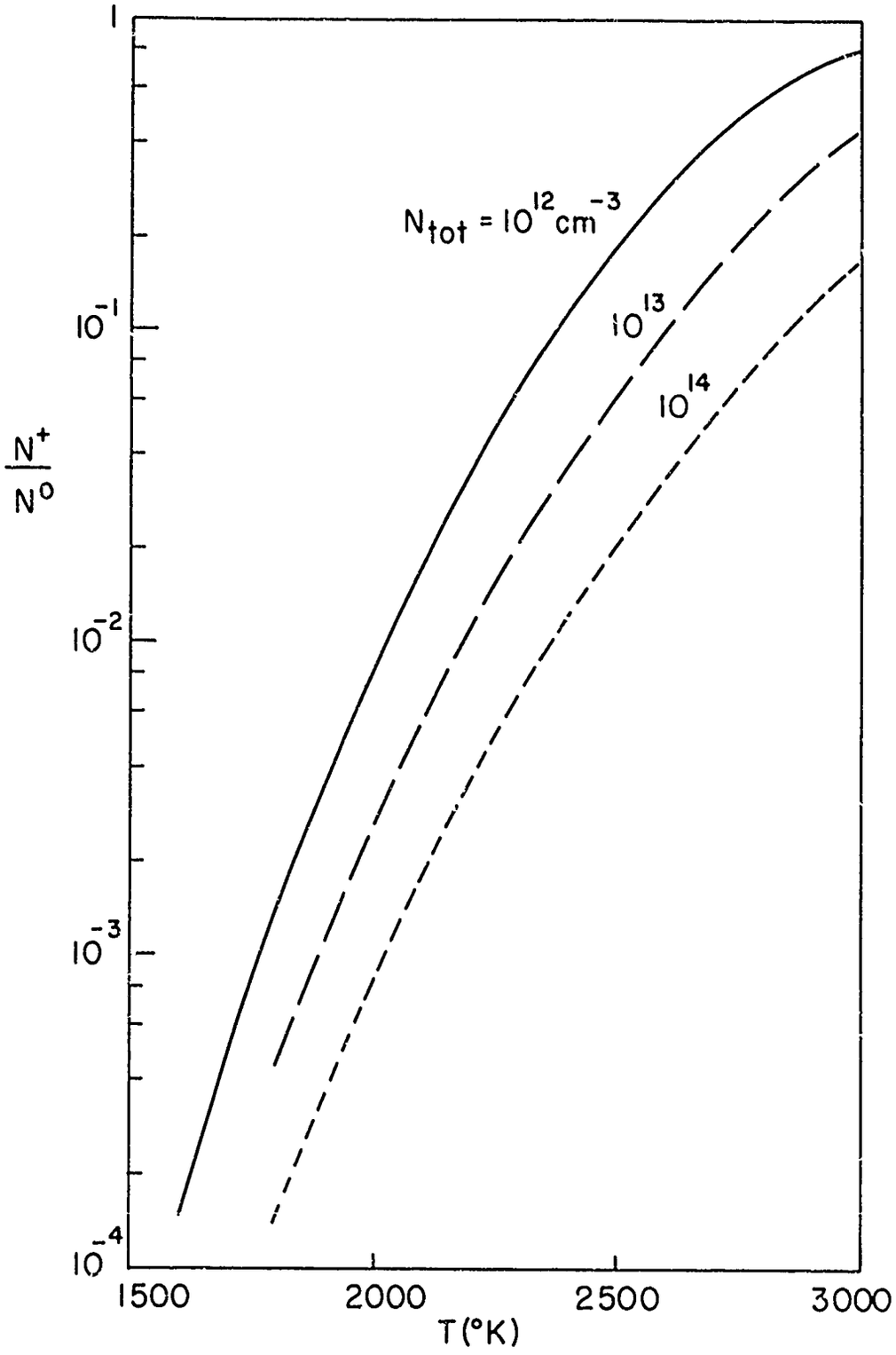

Figure III-3. Equilibrium Ratio of Singly Ionized (N^+) to Neutral Barium (N°). Higher Ionization Stages are Neglected.

Further calculations will be made in the next contract period to take into account the different stages of ionization of atoms of interest for studying with the CO_2 laser. The result of these calculations coupled with a survey of suitable compounds of these atoms will be very useful in determining a good target material for study with the CO_2 laser.

C. ESTIMATE OF LINE RADIATION

In this section we use the results on the thermal populations of the levels of sodium as well as empirical measurements of evaporation rate to make an estimate of the amount of power radiated into the sodium D lines by the plasma produced by irradiation of glass with a carbon dioxide laser.

In what follows we calculate the amount of power radiated into the sodium D lines by sodium atoms evaporating from soda lime glass in the form of an ordinary microscope slide. This calculation was made for glass because the rate of evaporation of the glass is easily measured by measuring the time that is required to pierce a hole through the microscope slide. Also, since this type of glass contains approximately 15% sodium oxide, it seemed like a good matrix from which to obtain thermally excited sodium atoms to determine the feasibility of measuring the plasma temperature from discrete-line emission. The radiated power is calculated as follows: The glass is assumed to evaporate as a compound at a temperature which is estimated from the color of the optical emission to be at least 1200°C (1500°K). From the experimentally determined evaporation rate and the known composition of the glass, the rate of evaporation of sodium atoms is determined. It is assumed that the plasma is not heated directly by the laser and cools rapidly by expansion. Therefore, a sodium atom only contributes once to the emission from the plasma. This last assumption may be too pessimistic, but by making it we will obtain a lower bound for the amount of power available in the sodium D lines.

The rate of evaporation used in this calculation was obtained as follows: The beam from the CO_2 laser with a total output of approximately 20 watts was focused on a one millimeter thick microscope slide using a ten centimeter focal length lens made of Irtran-2. A 0.5 millimeter diameter hole was evaporated through the full thickness of the glass in approximately one minute. From the above we determine a material removal rate of 3.25×10^{-6} cm^3/sec, and using the density of 2.85 grams/cm^3, a mass evaporation rate of 9.3×10^{-6} grams/sec is obtained. Assuming a soda (Na_2O) content of ten percent in this glass, the evaporation rate of sodium atoms is found to be 6.9×10^{-7} grams/sec. Using the atomic weight of 3.8×10^{-23} grams/Na atom, the evaporation rate for sodium atoms is

$$R_{Na} = 1.8 \times 10^{16} \text{ Na atoms/sec.}$$

Using an evaporation temperature of 1500°K and assuming complete dissociation of the sodium oxide, one obtains for the thermal velocity of the sodium atoms $V_{Na} = 7.4 \times 10^4$ cm/sec. From the thermal velocity, the known cross section and the atomic evaporation rate, one can find the density of sodium atoms near the surface of the glass. Assuming linear expansion perpendicular to the glass surface, the density would be 3×10^{14} Na atoms/cm^3. This density will be useful in the future for estimating heating rates of the plasma by the Q-switched laser pulse.

Now, assuming that each atom radiates only once as it leaves the surface with a thermal energy characteristic of the surface temperature, the power radiated by the sodium would be given by

$$P = R_{Na} \, h \nu \, N$$

where P is the radiated power, R is the atomic evaporation rate, h is Planck's constant, ν is the frequency of the emission, and N is the fractional population of the upper state of the transition.

For a temperature of 1500°K, the fraction of the total number of sodium atoms in the $^2P^o$ levels is found from Figure III-2 to be 2.5×10^{-7}. Use of the above quantities in the expression for the power gives P(1500°K) = 1.5×10^{-9} watts.

Assuming that the radiation is emitted isotropically, an f/4 spectrometer is able to collect $P/4\pi \times 16$ watts or 7.5×10^{-12} watts. If we were to assume that evaporation took place at 1000°K, instead of the assumed 1500°K, and that all the measured quantities remained constant, then the population of the $^2P^o$ levels would be 7.5×10^{-11} and the corresponding power intercepted by a spectrometer would be 2.25×10^{-15} watts. Thus, while the power received by the monochromator at the evaporating temperature of 1500°K would be a resonable power to detect using a photomultiplier and a phase sensitive detector, the amount of power available from evaporation at 1000°K would be very difficult to detect. These considerations point out the desirability of using as much power output as possible from the laser as well as using a target with a high vaporizatior temperature to increase the thermal population of the excited states.

We have checked experimentally the feasibility of measuring line radiation from the plasma produced when glass is evaporated by focusing the output of the CO_2 laser on it. A Perkin Elmer model 99-G monochromator with an aperture of f/4 was used to detect the radiation emitted by a target of soda lime glass. A photomultiplier with an S-11 photosurface was used as the detector. The output of the photomultiplier was fed directly into an EMC phase sensitive amplifier. The reference signal for the amplifier was provided by using a 13 cycle chopper with an optical pickup inside the laser cavity. Figure III-4 shows a spectrum obtained from the soda lime glass. It shows strong line radiation at the 5900 Å position of the sodium D lines which is considerably larger than the continuum background. The spectrum

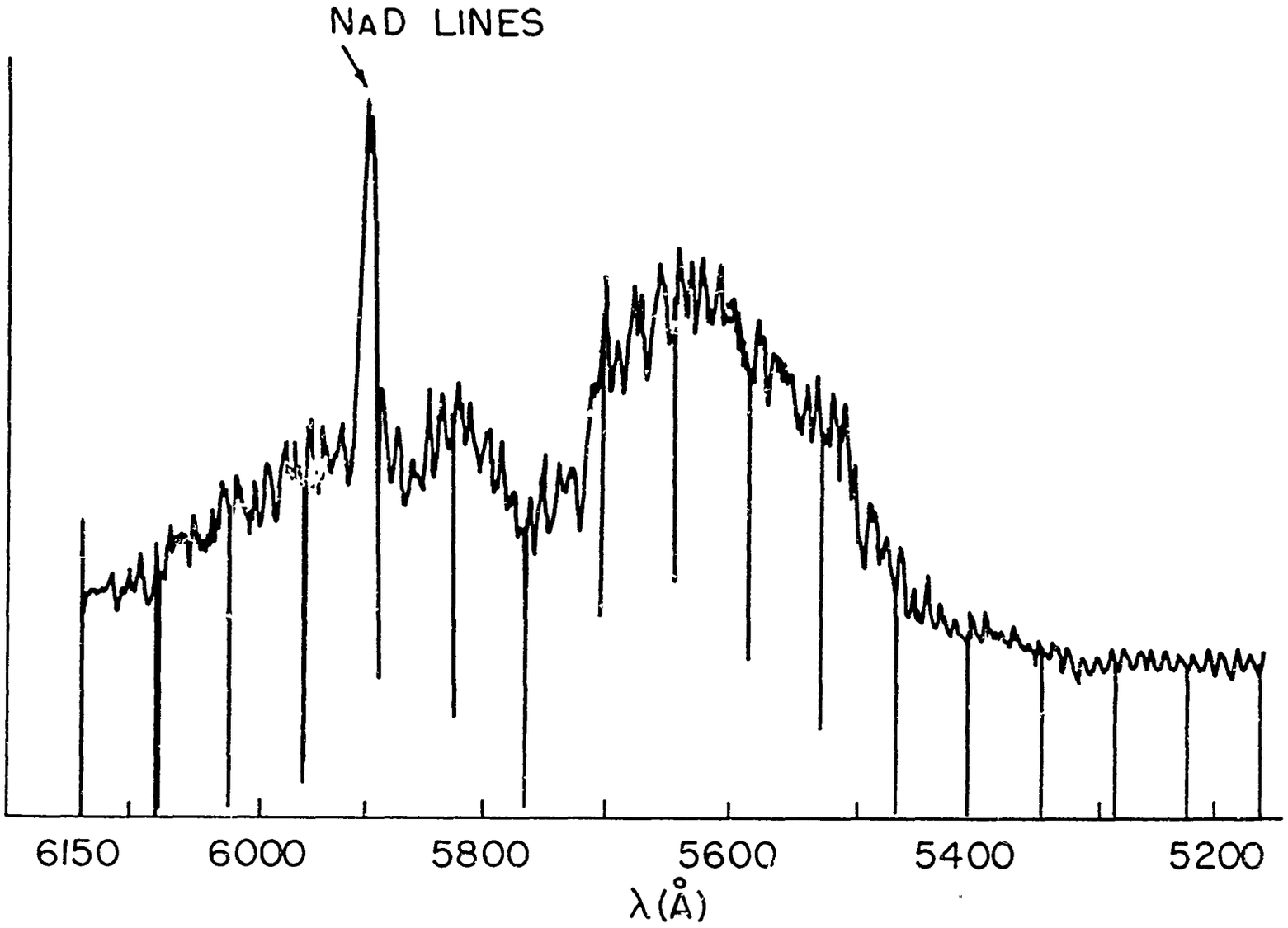

Figure III-4. Optical Emission from Soda Lime Glass Heated with CO_2 Laser. Strong Lines are Sodium D Lines. There are Several Overlapping Grating Orders Present.

is only to be taken as a qualitative indication of the detectability of the sodium D lines at the levels of irradiation indicated, and not a quantitative measure of the amount of power available since there are a number of overlapping grating orders present in the spectrum to which the photomultiplier is sensitive.

From the previous considerations of this section and the relatively large signal from the sodium D lines in Figure III-4, one concludes that the temperature of the material evaporating from the surface is probably in the neighborhood of 1500°K.

There are several comments that should be made about the experimental measurements on the spectrum from glass. First, it is found that the intensity of the sodium D lines from a glass target decays very rapidly. Typically, a strong signal from the D lines can be observed for less than one minute during irradiation of the glass and then the signal disappears. The decay seems to be associated with the rapid evaporation of the sodium oxide, leaving a compound which is poor in sodium. All the glasses tested so far suffer from this problem, and therefore will probably not be good candidates for target materials to make measurements over extended periods of time.

Second, while sodium as well as the other alkali metals have strong sharp lines in their first (neutral) spectrum that can be used for temperature measurements, the second spectrum corresponds to a noble-gas-like electron configuration whose excited levels lie at very high energy. Therefore, they will be difficult to populate at reasonable temperatures. This feature of the alkali metals makes them a little less attractive for the measurements of the effect of Q-switching a second pulse on the plasma because of the fact that it will be difficult to detect spectroscopically the ionized species. From this point of view, it appears that alkaline earth metals, especially barium, would be better suited for spectroscopic measurements of plasma heating.

However, since we are not familiar with the ability of the laser to produce high energy ions of barium, we must give cautious consideration to the choice of material. We will devote some effort in the forthcoming months to choose a suitable target as well as a suitable atom on which to make spectroscopic measurements.

The conclusions arrived at from examination of several possible target materials are the following: a) Glasses, while attractive because they have strong absorption at 10.6 microns and a fairly large sodium content, will probably not be good target materials to use for our measurements due to the rapid evaporation of the sodium. b) From the point of view of the spectroscopic measurements it would be more desirable to use alkaline earth metals as the atoms in which measurements were made. However, because of our lack of experience with heating this type of atom using lasers, we may have to reconsider the advisibility of these materials. c) Because of the rapid increase of the thermal population of the excited states that give rise to the radiation with temperature, it is desirable to use targets that have very high vaporization temperatures so that a large fraction of the evaporating atoms will be in excited states; and d) As a result of the previous considerations, a laser with as high an output as compatible with other practical considerations should be used. The effort in the CO_2 laser work in the first half of the next contract period will be spent primarily in choosing a suitable target material and in putting in operation a larger laser capable of an output of at least 60 watts in order to be able to evaporate materials with high vaporization temperatures. The emission spectra of these materials will be studied first under excitation by the output of the continuous laser. Later, changes in the optical spectrum under irradiation by a Q-switched laser will be examined.

SECTION IV

PICOSECOND PULSES AND DAMAGE IN TRANSPARENT MEDIA

We have begun an experiment to investigate the possibility of picosecond pulses being present in the output of our Q-switched laser. Such pulses were reported as being a general characteristic of Q-switched lasers [11] and have even been observed in non-Q-switched lasers. [12] The method of measurement [13] is to allow the laser beam to enter a solution of dye which fluoresces when excited by a wavelength lying between the ruby laser wavelength and half the ruby laser wavelength. Then two photon absorption will produce fluorescence but one photon absorption will not. Such a dye suitable for the ruby laser is 9, 10 diphenylanthracene. If the laser pulse is made up of a sequence of mode locked pulses, when the beam is reflected back on itself through the dye by a mirror at the end of the dye cell, the positions at which the incoming and outgoing picosecond pulses overlap will be marked by a brighter fluorescence, since the fluorescence is proportional to the square of the light intensity. Thus, regions in which pulses overlap will give a fluorescent intensity four times as great as the region in which no overlapping occurs. This should be distinguishable in photographic recordings of the fluorescence.

If such a phenomenon is occurring in our laser, it is important to know it, since this will change the estimates of the peak flux density used in previous theoretical analyses of the production of high energy ions. The setup for performing these measurements has the dye cell located at one end of an optical bench, and the laser on the other. See schematic diagram in Figure IV-1. As of the time of this writing, no definite data has yet been obtained from this system, but we expect this to be an important experiement in interpreting other results.

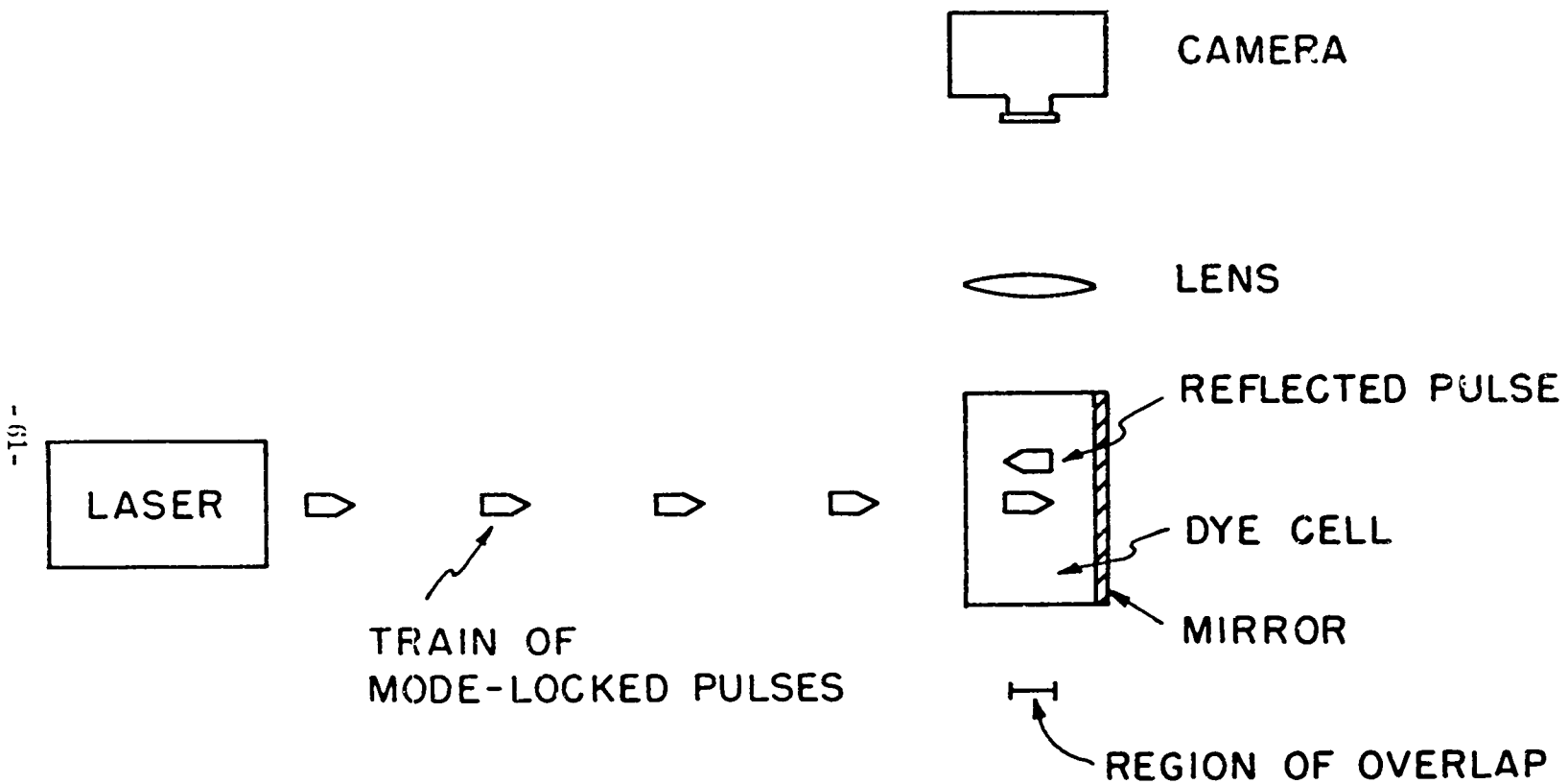

Figure IV-1. Arrangement for Measurement of Picosecond Pulses in Laser Output.

If picosecond pulsing is generally present in high power laser outputs, it can, in particular, explain the damage produced in transparent materials. Although stimulated Brillouin scattering and an associated hypersonic wave has been often suggested as the source for laser induced damage in transparent materials, [14] quantitative estimates of the pressure wave produced by the hypersonic phonons indicate that the pressures are too low to produce damage. The net electrostrictive pressure p is given by [15]

$$p = -\gamma E^2/2$$

in MKS units where $\gamma = \rho d\epsilon/d\rho$ is the electrostrictive coefficient (of the order of 10^{-11} MKS units); with ρ the density of the material and ϵ the dielectric constant. For a damage threshold around one gigawatt/cm^2, a typical value, this leads to a calculated pressure of 10^6 dynes/cm^2. This value is much below the dynamic pressure at which damage should be produced in glass.

In an effort to explain these phenomena we have also studied damage in glass. Figure IV-2 shows a picture of damage produced by a normal ruby laser pulse in a silicate glass. Damage is present as cracks, bubbles, and fractures in the interior of the glass. Typically there is a fracture plane oriented at an oblique angle to the direction of propagation of the laser beam. If picosecond pulses play a role in the production of such damage, the pressure produced in a hypersonic wave could be much higher than that calculated above on the basis of the average flux density contained in the pulse. Thus, experimentally, we should be able to observe damage when picosecond pulses are present, but no damage when they are not present. This is the dypothesis which we shall test experimentally, if it is shown that our laser exhibits picosecond pulsing. By controlling the number of modes in the laser but at the same time making sure that a constant average flux density is maintained at the focal point of the lens, the picosecond pulsing can be eliminated. If the hypothesis is correct, damage should not be produced even though the average flux density is the same.

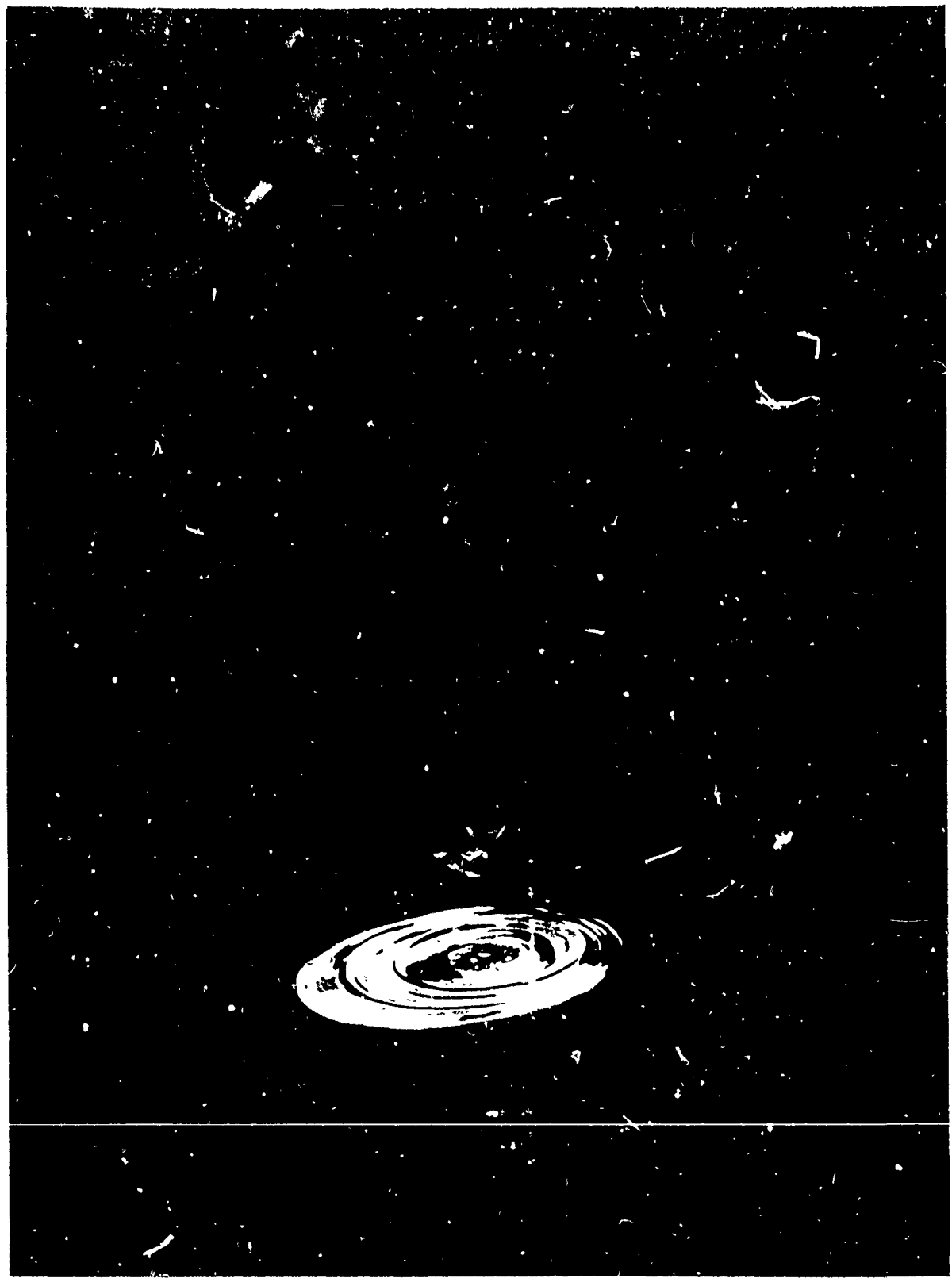

Figure IV-2. Damage in Glass Produced by a Non-Q-Switched Laser Pulse. Laser Beam was Incident from the Left. Fracture Planes are Visible. Largest Fracture is about 3mm in Diameter.

SECTION V

CONCLUSIONS

This report has emphasized interpretation of the data obtained in the hemispherical interaction chamber. It is apparent that the results from the interaction chamber indicate a greater complexity in the blowoff material than was anticipated when the chamber was designed. The design considerations were based on phenomena observed in the time-of-flight spectrometer. Apparently there is another range of phenomena which the time-of-flight spectrometer was not well designed to observe, but which play an important role in the results obtained in the hemispherical interaction chamber. In particular, it appears that there is a large amount of ion production, approximately 10^{13} -10^{14} ions per laser pulse, which expand as a neutral plasma. The temperature of the plasma is of the order of 10 eV. In contrast, the time-of-flight spectrometer measurements indicated about 10^{9} ions per pulse with ~200 eV energies, traveling essentially as individual charged particles. We may hypothesize that there is more than one group of particles produced in a laser-surface interaction, and that the time-of-flight spectrometer is well adapted to measuring the smaller number of high energy ions and the interaction chamber responds better to the more copious lower energy ion production.

The main experimental conclusions reached in this report are the following: The emitted material does not expand isotropically, but has an angular distribution as described earlier, with a maximum normal to the target. The angular distribution does not appear to be dependent on the direction of polarization of the laser beam. It appears that the signals in the hemispherical chamber are produced by a mixture of phenomena including direct charge collection from a small amount of uncompensated charge, and also from secondary electron emission produced by bombardment of the various surfaces by the neutral molecules and ions traveling from the target.

As a result of these conclusions, it will be necessary to re-examine the results which we obtained earlier in theoretical calculations on heating of the blowoff material by absorption of laser radiation in the inverse Bremsstrahlung process. In particular, the present results indicate that the total ion density may be higher than the value that was used in the earlier calculations which yielded essentially negative results. Moreover, the heating would have to proceed only to a temperature of approximately 10 eV. As we saw in a previous report,[6] the shapes of the emission pulses can be well explained by assuming a relatively modest amount of heating followed by an adiabatic free expansion of the heated material. The future work involving the absorption of ruby laser light in the blowoff material should be a critical one in studying the dynamics of heating.

It will be necessary to perform additional work to compare the results obtained in the interaction chamber with those in the time-of-flight spectrometer. Although the data obtained from the interaction chamber can be consolidated into a single picture, the picture does not necessarily agree with that obtained from the time-of-flight spectrometer. We shall therefore, consider further whether the discrepancies result from the different modes of operation of the two instruments and possibly from different sensitivities for detection of different groups of particles.

Another conclusion involves the suitability of the carbon dioxide laser for use in this laser effects work. Repetitive pulses at kilocycle rates with peak powers in the kilowatt range can be obtained from Q-switched CO_2 lasers in a single mode which can be focused to an area of the order of 10^{-4} cm^2, yielding a flux density of the order of 10 MW/cm^2. Since the coefficient for inverse Bremsstrahlung is much higher at a wavelength of 10.6 microns than at the wavelength of 6943 Å, and since the repetitive nature of the pulsing permits easier alignment and positioning and allows the use of phase sensitive techniques in processing the data, the CO_2 laser is suitable for use in the experiment on absorption of laser light in the blowoff material. Preliminary

results given in this report also indicate that optical investigations of the blowoff material produced by a CO_2 laser are promising. The relative intensities of the emission lines from different states of ionization can be used directly to derive the temperature of the blowoff material. Thus, the use of the CO_2 laser should provide a probe on the dynamics of the heating of the plasma and should also provide more accurate measurements because of the repeatability of the pulse shapes.

Finally, an investigation into the role of picosecond pulses and the possible existence of these pulses in our ruby laser appears to be necessary in order to form an adequate interpretation of our experimental results. Possibly picosecond pulses may also serve to provide a better quantitative understanding of the nature of damage in transparent materials. No experimental data is yet available on these points, but we shall pursue them in the next report period.

REFERENCES

(1) "Mechanisms of Laser-Surface Interactions," by J. F. Ready, E. Bernal G., L. P. Levine, Final Report to Ballistic Research Laboratories on Contract DA-11-022-AMC-1749(A), March 1965. (AD-467,867)

(2) IBID, Semi-Annual Report on Contract DA-11-022-AMC-1749(A) Mod.2, November 1965. (AD-477,231)

(3) IBID, Final Report on Contract DA-11-022-AMC-1749(A) Mod.2, May 1966. (AD-636,680)

(4) IBID, by J. F. Ready and E. Bernal G., Semi-Annual Report on Contract DA-18-001-AMC-1040(X), December 1966. (AD-645,473)

(5) IBID, by J. R. Ready, E. Bernal G., and L. T. Shepherd, Final Report on Contract DA-18-001-AMC-1040(X), May 1967. (AD-654,524).

(6) IBID, Semi-Annual Report on Contract DA-18-001-AMC-1040(X), Mod. No. 1, November 1967. AD666 245

(7) A. F. Haught and D. H. Polk, Phys. Fluids 9, 2047 (1966).

(8) Y. Takeishi and H. D. Hagstrum, Phys. Rev. 137, A641 (1965).

(9) H. R. Griem, "Plasma Spectroscopy," McGraw-Hill, New York (1964).

(10) C. E. Moore, Atomic Energy Levels, NBS Circular 467, U.S. Government Printing Office, Washington, D.C.

REFERENCES (Continued)

(11) M. A. Duguay, S. L. Shapiro and P. M. Rentzepis, Phys. Rev. Lett. 19, 1014 (1967).

(12) S. L. Shapiro, M. A. Duguay, and L. B. Kreuzer, Appl. Phys. Lett. 12, 36 (1968).

(13) J. A. Giordmaine, et. al., Appl. Phys, Lett. 11, 216 (1967).

(14) C. Guiliano, Appl, Phys. Lett. 5, 137 (1964).

(15) A. Yariv, Quantum Electronics, Wiley (1967), Ch. 25.

UNCLASSIFIED

Security Classification

DOCUMENT CONTROL DATA - R & D

(Security classification of title, body of abstract and indexing annotation must be entered when the overall report is classified)

1 ORIGINATING ACTIVITY (Corporate author)	2a. REPORT SECURITY CLASSIFICATION
Honeywell, Inc Corporate Research Center Hopkins, Minnesota 55343	Unclassified 2b. GROUP

3 REPORT TITLE

MECHANISMS OF LASER-SURFACE INTERACTIONS

4. DESCRIPTIVE NOTES (Type of report and inclusive dates)

Final Report

5. AUTHOR(S) (First name, middle initial, last name)

J. F. READY, E. BERNAL G., AND L. T. SHEPHERD

6 REPORT DATE	7a. TOTAL NO. OF PAGES	7b. NO. OF REFS
May 1968	74	15

8a. CONTRACT OR GRANT NO.	9a. ORIGINATOR'S REPORT NUMBER(S)
DA-18-001-AMC-1040(X) b. PROJECT NO. c. d.	9b. OTHER REPORT NO(S) (Any other numbers that may be assigned this report)

10. DISTRIBUTION STATEMENT

This document has been approved for public release and sale; its distribution is unlimited.

11. SUPPLEMENTARY NOTES	12. SPONSORING MILITARY ACTIVITY
	Commanding Officer USA Aberdeen Research & Development Center Aberdeen Proving Ground, Md. 21005

13. ABSTRACT

This report describes extensions of measurements of particle emission produced in the interaction of high power laser radiation with absorbing surfaces. Most of the experimental work in this report period involved the use of a hemispherical interaction chamber with collectors around the periphery. A multiplier detector and a bipolar detector have been employed in addition to the ordinary disc collectors used previously. The experimental results for a tungsten target and a laser flux density of the order of 50 megawatts/cm^2 indicate that the blowoff material consists of a mixture of neutral molecules and of a plasma containing approximately 10^{13} to 10^{14} electons and ions. Secondary electron emission from the collector surfaces bombarded by the incident heavy particles is important in producing the observed signals. Temperature of the expanding material is of the order of 10 eV. Additional work has been devoted to measuring the optical emission from glass samples heated by a CO_2 laser beam and also to an investigation of the possible presence of picosecond pulses in our laser output.

DD FORM 1 NOV 68 1473 REPLACES DD FORM 1473, 1 JAN 64, WHICH IS OBSOLETE FOR ARMY USE.

UNCLASSIFIED

Security Classification

14. KEY WORDS	LINK A		LINK B		LINK C	
	ROLE	WT	ROLE	WT	ROLE	WT
Laser Damage Plasma Mechanisms						